analytical chemistry

Review

pubs.acs.org/ac

Recent Developments in Paper-Based Microfluidic Devices

David M. Cate,[†] Jaclyn A. Adkins,[‡] Jaruwan Mettakoonpitak,[‡] and Charles S. Henry*[,†,‡]

[†]Department of Biomedical Engineering, Colorado State University, Fort Collins, Colorado 80523, United States

[‡]Department of Chemistry, Colorado State University, Fort Collins, Colorado 80523, United States

CONTENTS

Paper has been used as a substrate material in analytical testing for centuries, with scientific reports dating back to the early 1800s with litmus paper.[1] As a substrate material, paper (and related porous hydrophilic materials) has many unique advantages over traditional device materials including power-free fluid transport via capillary action, a high surface area to volume ratio that improves detection limits for colorimetric methods, and the ability to store reagents in active form within the fiber network. As a result of these benefits, paper has been used in applications ranging from spot tests for metals[2] and paper chromatography[3] to lateral flow immunoassays.[4] Paper as a substrate material for *microfluidic* assays was largely ignored, however, until 2007 when Martinez et al.[5] reported the first microfluidic paper-based analytical device (μPAD) for chemical analysis. The unique aspect of this seminal work lies in the use of a hydrophobic (photoresist in this case) patterning reagent to define hydrophilic flow channels for directing sample from an inlet to a defined location for subsequent analysis. This simple yet elegant development led many to realize paper as a substrate material for applications where low-cost and portability are critically important.[6]

This review focuses on recent developments in μPAD technology as it applies specifically to making chemical measurements in the time range of October 2012 to October 2014. During this time over 1 000 articles have been published in the field, making a full comprehensive review citing all papers impossible. As a result, we seek to highlight the papers we find to be most impactful for the field. We also limited our search criteria and resulting discussion to papers describing analytical measurements. In recent years, paper as a substrate material has been used more frequently for electronics as evidenced by a number of excellent reviews.[7,8] While many of these reports have bearing and importance to analytical measurements, they are not discussed here in interest of maintaining focus. The same is true of lateral flow immunoassays. Lateral flow immunoassays warrant a separate review based on their ubiquity and have been covered recently.[4] Finally, searches were done using a combination of Google Scholar, Web of Science, PubMed, and SciFinder. In addition, high impact journals were scanned for manuscripts that did not readily appear with standard search terms. Despite these extensive searches, we have, without a doubt, missed many excellent papers relating to paper microfluidics. For those papers missed, we apologize in advance.

THEORETICAL STUDIES

We first address developments on theoretical aspects of transport in paper devices focused on elementary imbibition

Special Issue: Fundamental and Applied Reviews in Analytical Chemistry 2015

Published: November 6, 2014

   dx.doi.org/10.1021/ac503968p | *Anal. Chem.* 2015, 87, 19−41

Scheme 1. Fabrication Schemes for Creating μPADs[a]

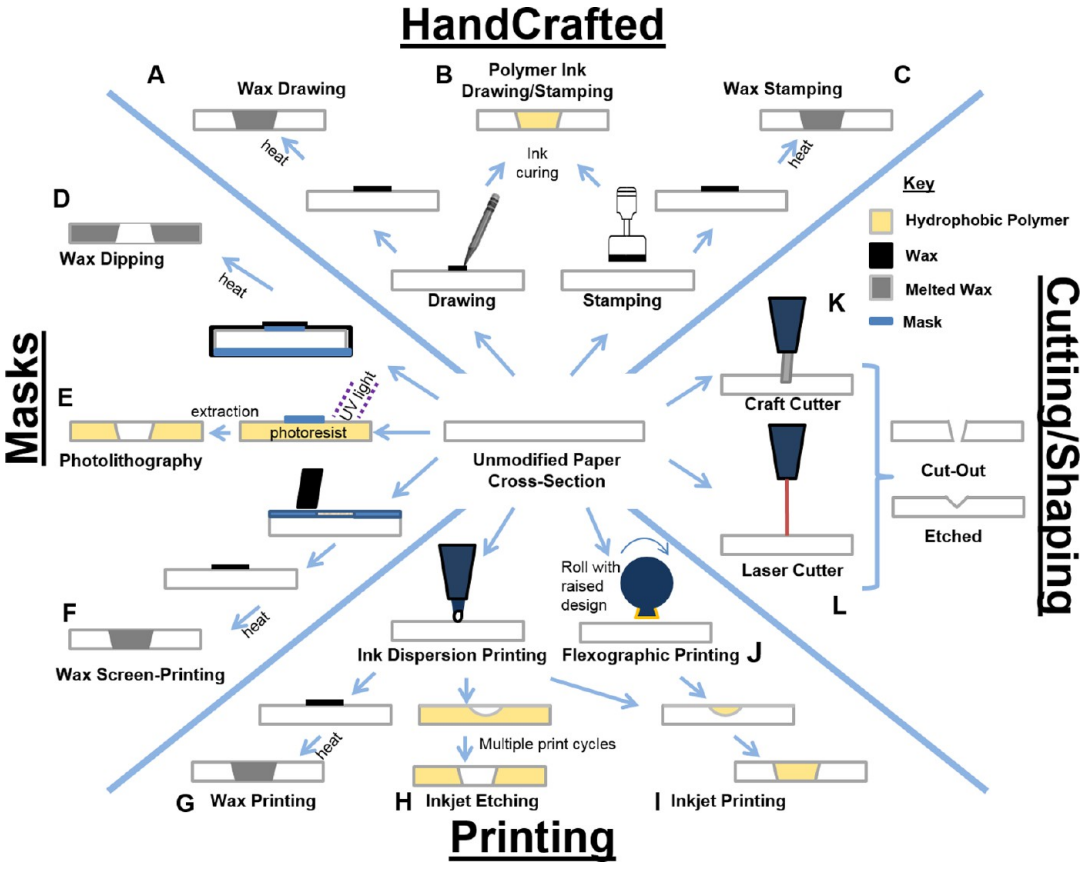

[a]Hand crafted devices fabricated using (A) Wax drawing, (B) polymer ink drawing or stamping, or (C) wax stamping. Masks were used to protect hydrophilic regions for (D) wax dipping, (E) photolithography, and (F) wax screen-printing. Fabrication techniques with ink addition printers used either (G) wax printing, (H) inkjet etching, (I) inkjet printing, or (J) flexographic printing. Cutting or shaping air boundaries or etching channels were performed by a (K) craft cutter or (L) laser cutter.

theory. The choice of paper material is entirely dependent on user application but can and will have significant and predictable impact on performance and fluidic transport. Consideration of substrate-analyte chemistry, wicking rate, material durability, and fabrication methods must be accounted for and are addressed in a series of excellent reviews.[6,9−12] For a more detailed discussion of theoretical flow, the reader is also encouraged to review additional papers on the subject.[13,14]

Wicking-based flow in capillary systems is considered laminar because fiber length scales and associated pores are typically less than 20 μm, resulting in low Reynolds numbers.[15−17] Spontaneous imbibition in porous media with constant cross section, and on short time scales, can be modeled by Darcy's law: $Q = -\kappa A/\mu L \Delta P$, where Q is the volumetric flow rate, κ is paper permeability, A is the cross-sectional area of the paper normal to flow, μ is the dynamic viscosity, and ΔP is the pressure drop occurring over a length L in the channel along the axis of flow. Darcy's law assumes kinetic energy can be ignored, the fiber cross-section is circular, and that capillaries are straight. Another assumption is that fluid properties remain constant. One-dimensional fluid flow in porous networks during wetting can also be approximated (to the first order) by the Lucas−Washburn equation assuming constant cross-section/cylindrical pores, negligible gravitational effects, chemical homogeneity, and unlimited reservoir volume:

$$x(t) = \sqrt{\frac{\gamma r t \cos\theta}{2\mu}} \quad (1)$$

where fluid with (liquid−vapor) surface tension γ and viscosity μ imbibes a distance x in time t, r is capillary radius, and θ is the contact angle between the fluid and capillary wall. Fluid penetration distance increases with increasing effective capillary radius. Washburn's equation holds for lateral flow as long as $x \ll z$ where z is the height of fluid in a vertical column when the negative force of gravity is equal to the positive capillary force.[18] The above equation is a first-order approximation of fluid transport, and it tends to overestimate lateral wicking speed with fluid penetration distance.[19] The variables not taken into account by eq 1 are the swelling that occurs in fibers during wetting, the increase in hydrodynamic resistance to flow during wetting, and that flow in paper networks is not straight (an assumption of the equation).[20] Other groups have since derived modified equations to improve predictive power by taking into account the forces of viscous drag, gravity, and inertia.[21,22]

Flow theory in tubes or porous systems with uniform cross-section is fairly mature; however, fewer attempts have been made to characterize flow in nonuniform or heterogeneous cross sections.[23−27] Indeed, it appears that simplified models assuming homogeneous porosity and/or tortuosity fall short of empirically predicting flow in complex porous networks with multiple layers, changes in geometry (e.g., wall curvature, widening or narrowing channels), or systems with more than

dx.doi.org/10.1021/ac503968p | Anal. Chem. 2015, 87, 19−41

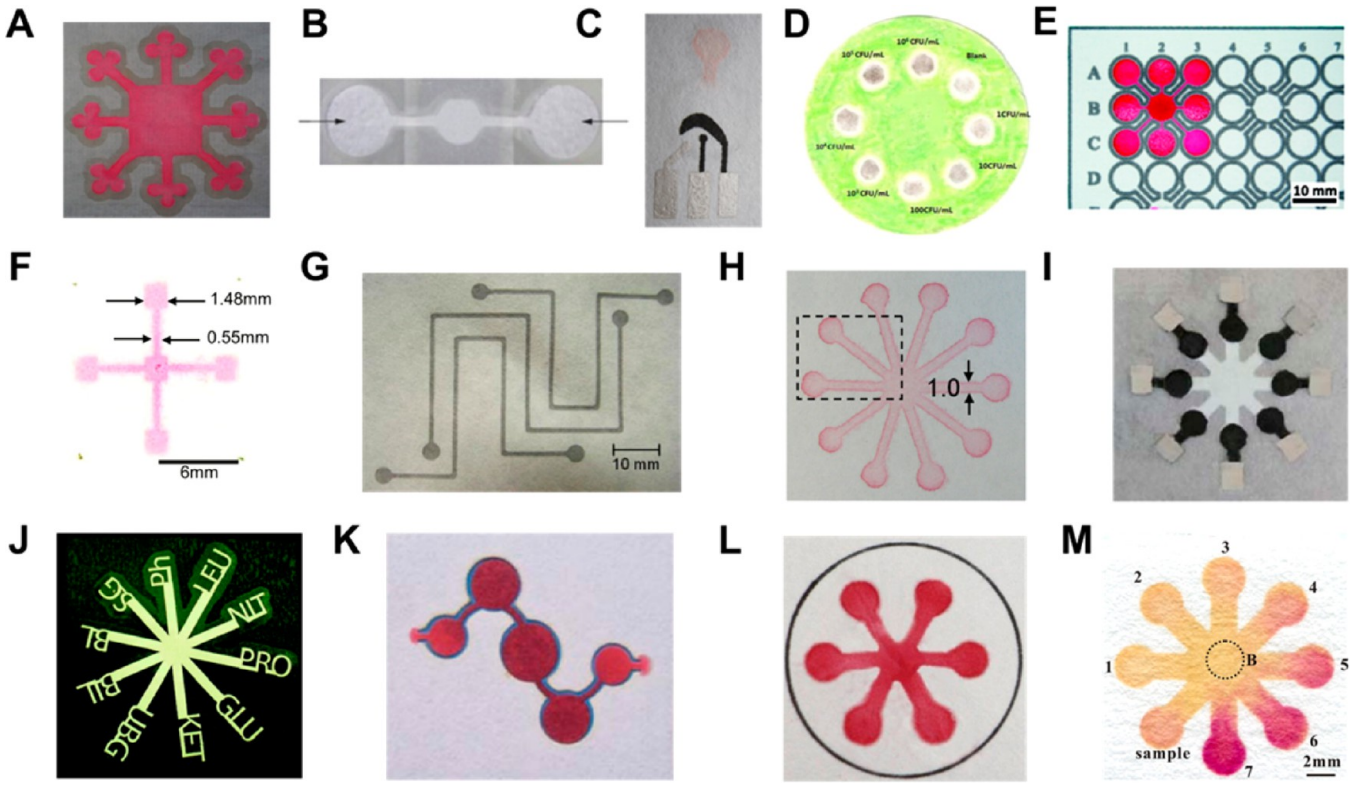

Figure 1. Example two-dimensional devices. (A) Wax stamping with movable type printing. Reprinted from ref 43. Copyright 2014 American Chemical Society. (B) Wax dipping. Reprinted with permission from ref 45. Copyright 2013 Elsevier. (C) Screen-printed wax device and electrodes. Reproduced from ref 39 with permission of The Royal Society of Chemistry. (D) Wax drawing through a stencil. Reprinted with permission from ref 47. Copyright 2014, with permission from Elsevier. (E) Wax printing. Reprinted from ref 40. Copyright 2009 American Chemical Society. (F) Inkjet etching of polystyrene in paper with toluene. Reprinted from ref 50. Copyright 2008 American Chemical Society. (G) Inkjet printing of AKD. Reprinted with permission from ref 51. Copyright 2010, with permission from Elsevier. (H) Flexographic printing of polystyrene. Reprinted from ref 55. Copyright 2010 American Chemical Society. (I) Photoresist patterning with screen-printed electrodes. Reprinted from ref 57. Copyright 2013 American Chemical Society. (J) Computer controlled knife cutting in nitrocellulose. Reprinted from ref 60. Copyright 2008 American Chemical Society. (K) Laser-cut hollow channels. Reproduced from ref 63 with permission of The Royal Society of Chemistry. Copyright 2013 The Royal Society of Chemistry. (L) Vapor-phase polymer deposition. Reproduced from ref 73 with permission of The Royal Society of Chemistry. Copyright 2014 The Royal Society of Chemistry. (M) Chemical modification with alkylsilane self-assembling and UV/O_3 patterning. Reprinted from ref 81. Copyright 2013 American Chemical Society.

one phase.[28−30] Studies show that accurately estimating capillary radius is paramount for any well-modeled description of wicking phenomena (e.g., mercury porosimetry).[31,32] Fang et al.[33] recently developed a model to describe the influence of pore size distribution on capillary flow in unidirectional fiber networks, an approach contrary to previous attempts in which an average pore radius for all fibers was assumed.[34,35] Energy balance equations were used to predict an effective capillary radius based on the principle that a reduction in free surface energy of any solid−liquid interface must be equal to the amount of energy needed to raise the liquid (in a vertical flow scenario). A new equation for predicting the effective capillary radius $r_{eff} = \sum_{r,min}^{r,max} r_i^2 f(r_i) / \sum_{r,min}^{r,max} r_i f(r_i)$, where r_i is the inner radius of a single fiber and $f(r_1)$ is the probability density function of capillary radius. Applying this estimate of r_{eff} in eq 1 better approximated empirical flow through complex fibrous networks compared to traditional estimates of capillary radius. Although estimating the pore size distribution can be laborious and requires optical visualization of the porous cross-section, this method described flow behavior with good accuracy as well as the deviation of flow behavior from eq 1. Two-phase flow at random geometrical interfaces was modeled by Wiklund et al.[29] to describe the effects of substrate microtopography such as surface roughness and pore size variation on flow. This work suggested that liquid was "pinned" at the corners (liquid contact angle >90°) when channel width expanded or at points of high curvature. Contact angle was also shown to vary depending on the medium.[36] Cai et al. developed a generalized model for liquid penetration in tortuous, noncircular capillaries using modified Hagen−Poiseuille and Laplace−Young equations.

Capillary flow in 1D and 2D tube models has been studied extensively, and researchers are beginning to understand asymmetric transport behavior, which is more indicative of flow behavior in paper-based sensors.[37] Numerical simulations are being developed for predicting three-phase-flow (liquid−solid−gas), and fundamental equations have been derived to account for the variation in pore distribution, fiber swelling, and path tortuosity. As μPAD technology progresses and devices becomes more complex, predicting flow behavior in three dimensions will be important. Moreover, in most paper sensors, fluid flow is in contact with a variety of solids (e.g., wax for defining channels). Numerical models that can account for the resistive forces from these effects could also prove important.

dx.doi.org/10.1021/ac503968p | Anal. Chem. 2015, 87, 19−41

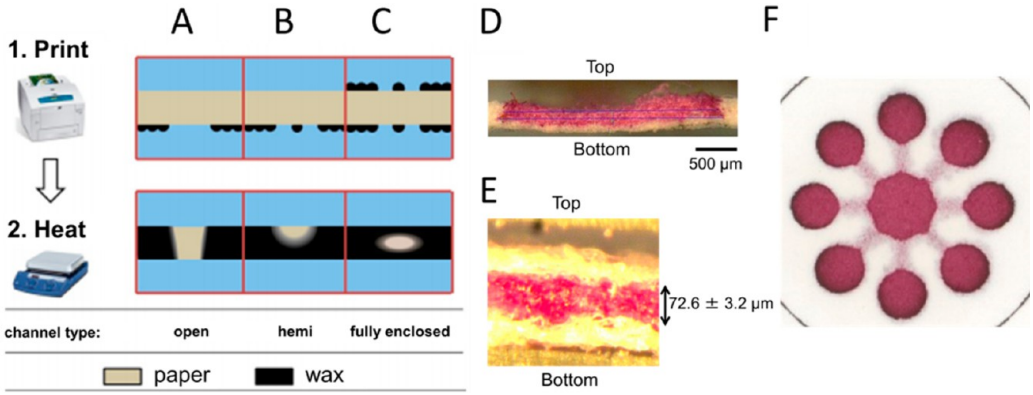

Figure 2. Example three-dimensional microfluidic devices. Wax printing schemes to create (A) open channels, (B) hemichannels, and (C) fully enclosed channels. Reprinted from ref 48. Copyright 2014 American Chemical Society. Resulting cross-section of inkjet printed (D) hemichannels and (E) fully enclosed channels. (F) Multiplexed device with hemienclosed wells attached to fully enclosed channels. Reproduced from ref 52 with permission of The Royal Society of Chemistry. Copyright 2013 The Royal Society of Chemistry.

FABRICATION

The earliest paper-based tests used paper manually cut into sections or strips and treated with a chemical reagent that reacted with an analyte to produce a colored product.[38] Although easy to fabricate, realization of more complicated devices with enhanced functionality has been pursued.[6] Common fabrication methods discussed here rely on either creating barriers within the paper itself or the selective cutting and/or removal of paper to create multifunctional μPADs.

Wax Patterning. The earliest μPADs were fabricated using photoresist to define flow boundaries;[3] however, the cost of photoresist and the potential for background reactivity makes this fabrication method less than desirable.[5,39] The limitations of photoresist methods led to the development of low cost fabrication methods that made use of wax and similar materials in lieu of photoresist. Creating barriers made from wax provides a low cost, easily accessible fabrication technology using relatively inert materials to contain fluid flow.[40] Wax, in particular, can be applied to paper using a variety of techniques and readily melts through the paper substrate with heat to create a three-dimensional barrier. Parafilm was one of the earliest materials used to pattern paper for simple colorimetric metal spot tests using a heated metal stamp (Scheme 1C).[41] More recently, de Tarso Garcia et al.[42] used a metallic stamp that allowed for single step fabrication of a dendrimeric channel structure for multiplexed colorimetric detection. A similar stamping method that combined movable-type printing technology with paper devices was also demonstrated for multiplexed design fabrication (Figure 1A).[43] These stamping methods allowed different combinations of design features to be printed simultaneously with minimal cost investment in capital equipment. A low-cost alternative using wax-dipping was reported by Songjaroen et al.[44,45] In this method, a metal mask covered the zones that were to remain hydrophilic and the system was dipped into molten wax (Scheme 1D and Figure 1B). The metal masks were held in place with a magnet. Another wax patterning technique used screen-printing methods for fabrication (Scheme 1F and Figure 1C). Screen-printing was done using standard emulsion-based screens and the applied wax was melted into the paper after printing.[39] Manual wax application through the screen resulted in low resolution and channel consistency; however, the cost of fabrication makes this method attractive. Wax drawing is an alternative to printing that has been used as a prototyping method or to add hand drawn features to wax printed devices (Scheme 1A and Figure 1D).[46,47] Although suffering from low throughput and resolution, these methods are low cost and can be done without expensive instrumentation. While the aforementioned methods are attractive, by far the most common fabrication method makes use of a commercially available office printer that uses a wax-based ink (Scheme 1G and Figure 1E).[40,46] The user is not limited by having to generate a new mask for different device designs, has the freedom to easily apply design changes, and can print devices within seconds. After printing, the wax printed pages are simply heated to melt the wax through the paper. The success of wax printing has led to the development of fabrication methods enabling creation of hemi- and fully enclosed channels within the paper (Figure 2A–C).[48,49] By printing either different thicknesses or amounts of wax, different size channels can be created.[49] Three-dimensional wax printing has allowed for more control of flow within paper as well as simplified generation of three-dimensional devices.

Inkjet Printing. An alternative to wax printing that continues to find interest is inkjet printing. The first example of device fabrication used toluene as the printed reagent to remove hydrophobic polystyrene that was prepatterned on the paper to create hydrophilic designs in a technique known as inkjet etching (Scheme 1H and Figure 1F).[50] More recently, inkjet printing has been used by Li et al.[51] to create barriers. Another reagent, alkyl ketene dimer (AKD), was printed onto paper and polymerized with heat to define hydrophilic regions (Scheme 1I and Figure 1G). In a similar method, UV curable inks were used as an alternative to more volatile and environmentally hazardous organic solvents typically used with inkjet methods (Scheme 1I).[52,53] Finally, an environmentally friendly approach was presented by Wang et al.[54] that used both inkjet etching and printing of sol–gel barriers in paper to fabricate devices. This type of barrier was able to withstand several types of organic solvents and surfactants that wax and AKD printed barriers could not. Inkjet printing can also be used to fabricate three-dimensional devices by incorporating hydrophobic reagents within the paper matrix itself, similar to wax printing. Covered channels were fabricated by printing thin layers across previously printed channels to create full enclosed or hemispherical hydrophilic regions (Figure 2D–F).[52] Inkjet printing also has the advantage of being the only reported fabrication technique able to not only

dx.doi.org/10.1021/ac503968p | Anal. Chem. 2015, 87, 19–41

fabricate flow channels but to also print reagents into testing zones with relatively high throughput and reproducibility.[50,52,53] However, a disadvantage to this technique is that inkjet printing usually requires several printed layers to generate devices and can cause problems with print resolution. Many of the solvents required to solubilize sensing reagents can be volatile and cause clogging or error in printed reagent amounts.

Flexographic Printing. Flexographic printing is another fabrication technique capable of high throughput production (Scheme 1J). Large commercially available flexographic printers capable of printing at speeds of greater than 300 m/min are used in industrial printing on a variety of substrates including paper and plastic. Currently there are only a few examples in the literature for flexographic printed μPADs. Hydrophobic barriers were flexographically printed on μPADs using a polystyrene ink dissolved in volatile organic solvents (toluene and xylene) by Olkkonen et al.[55] Depending on the solvent viscosity and vapor pressure and the polystyrene concentration, channels could be printed partially or completely through the paper within a few replicate layers of printing (Figure 1H). Poly(dimethylsiloxane) (PDMS) in a commercially available ink form was also used to flexographically print devices but required more replicate print layers to penetrate through paper than inkjet-printed PDMS.[56] Although flexographic printing is the fastest fabrication technique, it has several limitations. First, it requires a specialized flexographic printer as well as individual printing plates specific to the printer, limiting availability and design flexibility. Similar to inkjet printing, this method requires multiple printing steps to fully define channels, putting a premium on resolution and ultimately limiting reproducibility. Finally, this method can only print one reagent at a time. Despite these limitations, the use of flexographic printing, or other similar methods, will likely continue to grow in importance, as high-throughput fabrication becomes important for commercial applications.

Photolithography. Photolithography was first used to fabricate μPADs by Whitesides[5] and relies on UV exposure through a photomask of photoresist-saturated paper (Scheme 1E and Figure 1I).[57] Uncured photoresist is removed with solvent, leaving hydrophobic, cured photoresist barriers within the paper. In an attempt to create a similar fabrication technique capable of being performed in developing countries, sunlight was used instead of a UV lamp and hot plate to cure the photoresist. Paper was soaked in SU-8 photoresist, dried, sandwiched between black construction paper and the photomask, and cured. In a variant of this approach, Martinez et al.[58] patterned SU-8 using a pen without a photomask, further simplifying the process (Scheme 1B). Like any hand drawn fabrication method, however, creating reproducible designs is challenging. Recently, trichloromethane-diluted photoresist was used by OuYang and co-workers[59] to decrease photoresist consumption and required drying time (<1 min). A downside to using photoresist is that it suffers from low mechanical flexibility and can crack or break with bending.

Paper Cutting and Shaping. Cutting and/or paper removal to create two- and three-dimensional μPADs has resurfaced as a popular means of device fabrication.[60−62] Two advantages of these methods are that no chemicals are needed to define flow boundaries, and the equipment is generally widely available and low cost. Because fabrication does not rely on the flow of wax, polymers, or solvents within paper for definition, there is greater precision in manufactured device barriers (measured standard deviation of fabricated channel widths for wax printing,[40] inkjet etching,[50] and laser-cutting fabrication[63] were ±45 μm, 50 μm, and 10 μm, respectively). However, because much of the material is removed, these devices suffer from low mechanical stability and rely on solid supports, increasing cost.[64] Besides using hand-held blades and hole punches to create devices,[62] craft knife cutting[60] and CO_2 laser cutting[61] have been used to improve precision, speed, and production volume.

Craft cutters rely on a computer controlled knife to cut paper. The knife is capable of cutting at different pressures and angles and varies depending on the application (Scheme 1K and Figure 1J).[60] A disadvantage to this method arises from the cutting action itself which can cause warping or tearing. Multiple passes at lower cutting forces can be used, however, to reduce damage. Adding a more durable backing to the paper can also reduce damage. Fenton et al. created μPADs by craft cutting nitrocellulose, but because it is very thin and easily torn, a polyester backing was required.[60] Other paper types have been explored.[64] Recently, craft cutting was used by Giokas and co-workers[65] to engrave open channels either perpendicular or parallel to the direction of flow in hydrophilic channels to decrease or increase fluid flow, respectively. These engraved channels have also been cut into omniphobic (both hydrophobic and oleophobic) paper, were sealed with tape to create enclosed channels, and an external pump was used to drive flow.[66]

Laser-cutting using a computer controlled CO_2 laser has been used in μPAD fabrication (Scheme 1L).[63,67,68] This technique is similar to using a computer controlled craft knife cutter but has the advantage of being able to cut through material in one pass without having to back the material for stability. The main disadvantage of this technique is the expense of a laser cutter ($450−$8 000) relative to a craft knife cutter ($65−$400). Like craft cutting, laser-cut devices have been shaped into multi-inlet dipstick tests for controlled reagent addition[61] and multiplexed sample analysis.[63] Although the majority of fabricated laser-cut devices are completely cut and removed from a sheet of paper,[61,69] Nie et al.[63] recently created laser-ablated hollow channels still partially attached to the bulk filter paper sheet (Figure 1K). An advantage to this technique is that an additional step to remove unused, excess material is no longer needed. This ablating process was also used to form hollow channels in polyester supported nitrocellulose without cutting through the polyester, and the polyester supported the hollow channel boundaries as well as the resulting paper frame around the outside of the device.[68] Embossing has been used recently as a way to shape channels in omniphobic paper.[70] Although embossing is simple and does not require expensive instrumentation to construct, fabricated devices are limited by the need for an external pump. This method requires that paper be hydrophobic; thus, it loses its ability to wick solution.

Other Fabrication Techniques. A few other less common techniques that have been used within the past few years include indelible ink stamping,[71] screen-printed PDMS,[47] lacquer spraying,[72] and vapor phase polymer deposition.[73] All of these techniques require masks or stamps to pattern the hydrophobic regions and protect the remaining hydrophilic regions in paper. The first of these techniques made use of commercially available indelible inks and used a PDMS stamp to press the ink onto the paper, creating a hydrophobic barrier (Scheme 1B).[71] Screen-printed PDMS is a similar process to wax screen printing (Scheme 1F) except PDMS ink is used instead of wax to pattern flow regions.[47] Unlike wax screen-

dx.doi.org/10.1021/ac503968p | Anal. Chem. 2015, 87, 19−41

printing, the PDMS ink completely penetrates through the paper prior to heat application. Acrylic lacquer polymerizes as it dries to produce a clear hydrophobic barrier. Hand painting lacquer around a mask was used to make hydrophobic barriers, but it was found that the penetration of lacquer under the mask edge could not be controlled and proved irreproducible on both Whatman No. 1 and No. 4 filter papers.[72] Spraying lacquer provided a more consistent and reproducible method for creating a hydrophobic barrier than painting. However, it was found that paper with small pores such as Whatman No. 1 (11 μm pores) prevented lacquer penetration through the paper, resulting in leaking. Whatman No. 4 filter paper (20−25 μm pores), however, allowed lacquer to fully penetrate the paper and create reproducible hydrophobic barriers with no leaking.

Vapor phase polymer deposition was first introduced as a method to incorporate functionality into paper-based devices by Kwong and Gupta[74] but has more recently been used to fabricate hydrophobic barriers using initiated chemical vapor deposition (iCVD).[73] In this method, monomer (hydrophobic dichloro-[2,2]-paracyclophane) was first vaporized in a vacuum to initiate radical formation and then polymerized within the paper using a mask to define hydrophobic (poly(chloro-*p*-xylene) regions (Figure 1L). An advantage of this fabrication technique is that it does not require solvents. The same iCVD technique has been used to create fluoropolymer barriers made of poly(1H,1H,2H,2H-perfluorodecyl acrylate).[75] Fluoropolymers have been used extensively due to their good chemical and mechanical stability but transition metal salts have been found to selectively inhibit polymerization. To create a μPAD using this chemistry, Cu(II) chloride was patterned in the channel zones and the monomer was deposited uniformly on the paper. After polymerization, the paper was washed with methanol and water leaving hydrophilic regions where the Cu(II) was deposited. Plasma polymerization of fluorocarbon, octafluorocylobutane, in paper has also been used to add hydrophobic fluoropolymer barriers to paper.[76] A photomask and plasma exposure were used on both sides of the paper to ensure polymer penetration through the paper. A final method for polymer modification of paper not requiring a vacuum or expensive instrumentation as with previous methods is based on the precipitation of hydrophobic, biodegradable polymer poly(hydroxybutyrate) (PHB). Cellulose paper saturated with PHB in chloroform was put into an ethanol bath, resulting in aggregation and precipitation of PHB onto the paper surface. The resulting hydrophobic paper is made hydrophilic by UV/O_3 exposure through a photomask to create flow channels.[77] Drawing using water-soluble ink and inkjet printing inks onto the surface of the paper was also used to create hydrophilic regions on the paper surface.[78]

Chemical Modification of Paper. While the majority of processes have used hydrophobic additives to create barriers, several techniques have used covalent chemical modification of the paper itself. Several reactions have been published that rely on reacting with functional groups in cellulose. As previously mentioned, AKD is one chemical modification method used to make paper hydrophobic.[51] AKD is added to the −OH groups in cellulose through an esterification reaction and hydrophobicity arises from the resulting addition of hydrocarbon chain moieties. Recently, Cai et al.[79] used trimethoxyoctadecylsilane (TMOS) reacted with −OH groups in cellulose to create hydrophobic regions. A paper mask saturated in TMOS was placed in contact with native paper and heat was used to evaporate and react the TMOS with the paper above the mask.

Masking UV light with photomasks has been used to either photochemically react polymers of different functionality with cellulose or to degrade already bound polymers. UV-irradiation was used to attach hydrophobic poly(methyl methacrylate) with 4-methyacryloxyloxybenzophenone to cellulose.[80] Benzophenone functional groups react with the aliphatic C−H groups in cellulose, resulting in covalent attachment and cross-linking. A photomask was used to leave regions of unreacted polymer in the paper that was extracted to create flow regions. Using this technique, however, required both sides of the paper to be exposed to UV-light to polymerize the polymer. He et al.[81] used octadecyltrichlorosilane (OTS) as a hydrophobic molecule to modify paper. OTS readily reacts with paper via a condensation reaction between the cellulose −OH groups and the OTS silane groups. UV-light in combination with ozone (UV/O_3) was used to selectively decompose the hydrophobic regions via photolysis, creating hydrophilic regions for flow (Figure 1M). Plasma modification to paper, however, usually requires a vacuum and bulky, expensive instrumentation, making it impractical for device fabrication in low resource settings. However, Kao et al.[82] fabricated a battery powered, portable, and flexible microplasma generation device capable of chemically modifying hydrophobic paper substrates including wax and fluorocarbon modified paper into hydrophilic regions under ambient conditions.

Three-Dimensional Devices. Fabrication of μPADs with multiple layers to form three-dimensional (3D) devices has been of interest because functionality can be added without increasing device size. Recently, two methods for 3D μPAD fabrication have been reported. The first method involves taking individually cut paper layers and stacking them (Figure 3, panels A and B).[83] The second technique involves folding layers of a device from a sheet of paper to form a device and is based on the practice of origami (Figure 3, panels C and D).[84]

Multiplexed analysis of a single sample was accomplished from two inlet ports that flowed to eight unique detection areas that were spotted with detection reagent (Figure 3B).[83] Stacking paper layers with splitting and connecting channels allowed solution to flow both vertically and horizontally through paper (Figure 3A). The device contained the necessary channels and functions on multiple layers, creating a footprint that was only limited by the detection zone and sample inlet. 2D devices would have required a substantially larger footprint to accomplish the same chemistry. 3D devices can also incorporate layers of functionality made from alternate materials such as membranes used to separate out interfering species in an analysis.[45] Different layers can also be used to incorporate different detection methods. As an example, traditional screen-printed electrodes on transparency film can be used as one detection layer and integrated with a device containing separate colorimetric detection layers.[85] The alternating layers of paper make it easy to incorporate functionality such as timed reactions[43] and sequential addition of reagent[86] while still maintaining a small footprint.

Sealing and Packaging. Although many devices fabricated for research and proof of concept purposes are simply open channel and testing zones, it is useful and sometimes necessary to consider packaging the devices. Sealing the devices, especially when reagents are stored in paper, is necessary to prevent device contamination and for long-term storage. Sealing has also been used to minimize or control solvent

dx.doi.org/10.1021/ac503968p | *Anal. Chem.* 2015, 87, 19−41

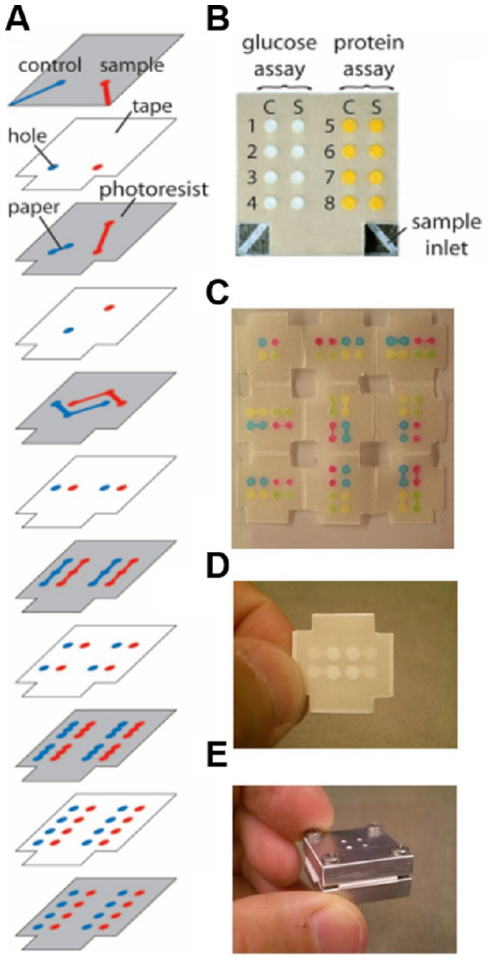

Figure 3. Three-dimensional device fabrication using (A) the cut-and-stack method. (B) Resulting device with eight spot tests for each sample inlet. Reproduced with permission from ref 83. Copyright 2008 National Academy of Sciences, U.S.A. An origami-folding technique was used to make 3D devices with (C) all device layers shown on a single sheet, and (D) the postfolded device with (E) a metallic holder for device operation. Reprinted from ref 84. Copyright 2011 American Chemical Society.

evaporation within devices, which can increase detection sensitivity.[87] Although adding plastic packaging increases the device cost, it also has the advantage of providing physical support and keeps the devices more mechanically stable. Several materials have been incorporated as both a support and as a sealant. Adhesive tapes have been used extensively to seal and package devices, especially since many are transparent and can be used as viewing windows into the device.[88] Tape is inexpensive and easily obtained.[83] Lamination sheets, another office or craft supply, have also been used as an easy method to seal devices between sheets of plastic using commercially available lamination equipment.[89] Heating lamination sheets to seal devices can be an issue with temperature sensitive reagents impregnated into the paper but can be avoided by using either self-adhesive lamination sheets[60] or selectively heating only around the edges of the devices.[90] One time-consuming step, however, when sealing devices is that holes must be cut or punched into any lamination/adhesive sheets prior to application, slowing the fabrication process and adding an additional alignment step. A potential problem with using adhesives with paper-based devices is that the adhesive could impact the chemical reactivity for detection and/or change paper wettability. Depending on the fabrication method, sealing can also be accomplished using the same materials used to create the hydrophobic regions. Both flexographic[55] and wax[48] printing have been used to create fully enclosed hemi- or enclosed channels within paper. Combinations of fabrication techniques have also been used to seal devices. For example, wax printing has been used to create the channels and inkjet-printed hydrophobic toner over the top and bottom of the paper was used to seal the channels and reagent storage areas.[91] These methods can be used to prevent direct contact and contamination of reagents within the paper-based device, while leaving only inlet and outlet regions exposed for sample addition and viewing results, respectively.

INCORPORATING FUNCTIONALITY

Paper is an excellent substrate for controlling fluid flow without external power and for confining liquids to specified regions. Unfortunately, the physical properties inherent with porous substrates offer limited control over fluid transport, especially regarding the rate and direction of flow. This renders many paper-based methods ill-suited for handling complex chemical matrixes or for performing multistep tasks. The earliest μPADs were incapable of complex functionality, limiting their impact in the analytical community. More recently, however, research groups have begun integrating functionality into μPADs for better liquid handling and autonomous operation within the device, opening new opportunities for μPADs as a viable alternative to traditional analytical methods.

Programming and Timing. One of the first demonstrations for controlling complex fluid flow was in 2010 by Martinez et al.[92] with the development of a three-dimensional μPAD incorporating single-use "on" buttons designed to direct the flow path. Strategically positioned gaps separated layers of paper and tape and then connected fluidic paths when pressed. This digital valve was capable of preventing flow completely until pressed. Single-use valves have limitations, but this work demonstrated the utility of programmable μPADs for prioritizing sample testing or for manually controlling timed reaction sequences. Several other groups reported additional methods for controlling fluidic transport, primarily by altering channel geometry.[13,15,93−95] Channel junctions that transition from narrow to wide experience a reduction in flow rate. Toley et al.[96] introduced another method for controlling flow by diverting it through a tunable cellulosic shunt placed in the flow path and in complete contact with the nitrocellulose substrate (Figure 4A). By tuning the length, width, and thickness of a shunt, the authors reported that flow could be delayed from 3 to 20 min with coefficients of variation under 10%.

Introduced in 2010,[93] fluidic barriers made of materials soluble in the carrier fluid have been demonstrated for controlling multistep processes. Sucrose is a common material for these barriers because it is inexpensive and readily abundant. Increasing the amount of sucrose increases the time delay for fluid to pass through a barrier from minutes up to hours.[97] A similar concept was applied to digital "on/off" switches by Houghtaling et al.[98] in which a bridge composed of soluble sugars (mannose or trehalose) wicks fluid through it until eventually dissolving and effectively shutting off flow completely (Figure 4B). By tuning the bridge material concentration and/or geometry, each bridge passed between

dx.doi.org/10.1021/ac503968p | Anal. Chem. 2015, 87, 19−41

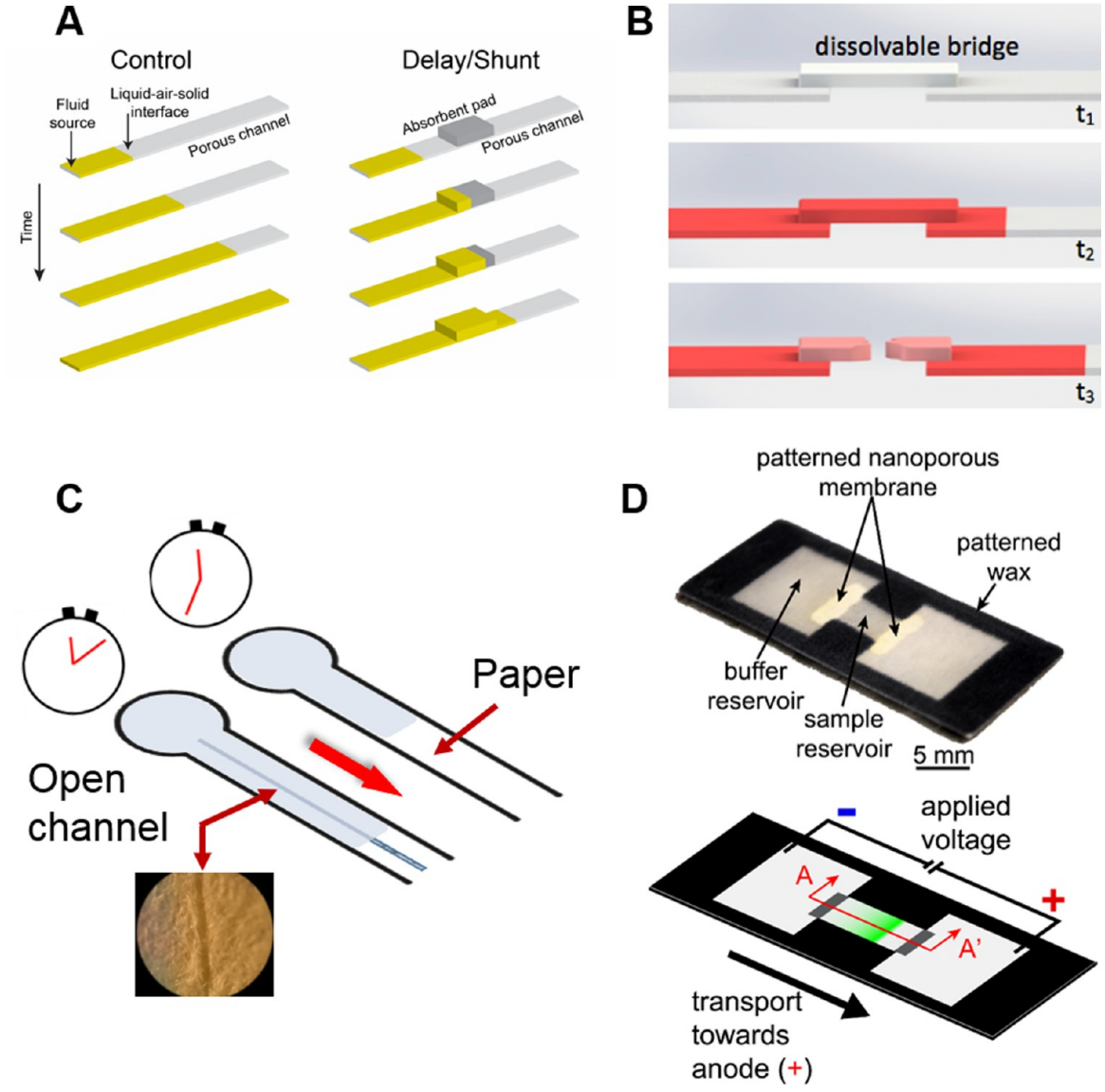

Figure 4. (A) Tunable paper shunts delay fluid flow by controlling shunt width, height, and placement in the porous channel. Reprinted from ref 96. Copyright 2013 American Chemical Society. (B) A dissolvable bridge functions as a digital "on/off" switch. Once the bridge dissolves in the carrier fluid, flow ceases. This valve is single-use only. Reprinted from ref 98. Copyright 2013 American Chemical Society. (C) Carving microgrooves into the flow path can accelerate flow (longitudinal grooves) or decelerate flow (latitudinal grooves). Reprinted from ref 65. Copyright 2014 American Chemical Society. (D) Nanoporous membranes are patterned in paper channels for directional transport analyte. Reprinted from ref 111. Copyright 2014 American Chemical Society.

10 and 80 μL. Jahanshahi-Anbuhi et al.[99] later developed a water-soluble pullulan film, which served in similar capacity.

Lewis et al.[100−102] coated hydrophilic zones with synthesized poly(carbamate) oligomers designed to depolymerize in the presence of H_2O_2, "switching" from water-insoluble to water-soluble. In this manner, the concentration of analyte is measured based on the time taken for depolymerization to occur in a paper zone relative to a separate control zone. The assay is complete once fluid wicks through pads containing green dye, which is placed at both target and control zones. Analytes of higher concentration lead to more rapid oligomer depolymerization; thus, the difference in time between the control and target zones is longer than for low analyte concentrations. Phase-switching is a very innovative method of detection because it only requires a device for keeping time (e.g., battery-operated timer, watch, cellphone), which are readily available in a point-of-care (POC) setting. Moreover, time-based assays are very sensitive; ∼femtomolar concentrations of biologically relevant enzymes have been measured.[103]

Razor-crafted μPADs have also been presented for controlling fluid delivery through porous channels (Figure 4C).[65] By cutting slits in the paper parallel or perpendicular to the flow direction, flow rate could be adjusted based on slit length, orientation, and number. Microchannels were carved into the substrate using a line plotter equipped with a knife blade, creating channel widths of 130 ± 20 μm, on average. When microchannels were crafted longitudinally (along the direction of flow), the time for reagent delivery from one end of the channel to the other decreased up to 60%, depending on channel length. Conversely, overall transport time was reduced by ∼40% if six microchannels were crafted perpendicular to flow. An advantage of these "subtractive" methods is they better accommodate small sample volumes because cellulose fiber is

dx.doi.org/10.1021/ac503968p | Anal. Chem. 2015, 87, 19−41

not added to the substrate. Additive methods increase sample retention in the filter network, thereby forcing sample volumes to increase in parallel.

A clever strategy for controlling flow in μPADs was developed by Renault et al.,[104] in which some cellulose was removed from the flow path by a craft cutter, consequently increasing the rate of liquid transport through paper. This strategy can be advantageous for several reasons. One, large particles have better mobility when less cellulosic material is present. Two, the rate of nonspecific adsorption is decreased. Three, if after removing most of the cellulose, a cover (i.e., tape) is sealed over the remaining void space to create an enclosed channel, resistance to mass transfer is dramatically reduced, and a single droplet can induce fast, pressure-driven flow. As a result, this strategy could be used to increase reagent delivery, which is a common problem for many paper-based sensors.

Multistep Processing. The trend toward increasing the functionality of μPAD assays starts with automating multistep processes. In 2011, Fu et al.[14] and Lutz et al.[105] investigated the sequential delivery of multiple reagents to a detection region by incorporating multiple constant-width sections of filter paper for each reagent addition step. Apilux et al.[106] created multiple flow paths of varying length, with different reagents in each path, to create a one-step automated sandwich ELISA assay. Hydrophobic barriers composed of dipropylene glycol methyl ether acetate (with 20% acrylic polymer) were printed for controlling flow. Baffles of the same material were added as well. The printed baffles essentially extended the flow path; more baffles effectively delayed flow. Li et al.[107] also demonstrated device control for multistep assays using magnetically timed "open/closed" single-use valves. Each valve was essentially a porous material (facial tissue) placed at the end of a magnetic cantilever. At time zero the valve was either placed down on the channel, creating a path for fluid transport across the valve ("closed" state) or it was raised above the channel which stops flow ("open" state). The cantilever was triggered by an ionic resistor, which was activated once flow from the inlet reached the resistor. The length of the timing channel was varied depending on the delay desired for on-chip processes. One limitation of this method is that in the proposed design, actuation of the cantilever is one-time-only, and the method for triggering the valve consumes large quantities of reagent. Moreover, this method requires a redesign of the timing channel for every new assay that requires a unique timing sequence.

To improve the portability, utility, and user-friendliness of μPADs, any necessary reagents can be included on the device, preferably in a dry state. There are several benefits of this: (1) the number of required user steps are reduced, (2) the complexity of shipping test kits is reduced because dry reagents are contained within the paper network, and (3) dry reagents are less labile in changing environmental conditions. Additionally, as demonstrated by Fridley et al.,[69] reagents dried in paper networks are amenable for multistep processing based on where and how reagents are deposited in devices. In their method, a μPAD was cut from nitrocellulose to form a single detection zone "downstream" from three paper side-channels that contained dry reagents and were a different length from the detection zone. All three channels were immersed in a carrier fluid simultaneously, and the reagents in the channels with the shortest overall distance from the detection zone arrived at the detection zone first. This controlled rehydration concept was demonstrated for the detection of malaria antigen, *Plasmodium falciparum* histidine-rich protein 2, where signal enhancing molecules were sequentially carried to the detection zone to enhance the detection signal ~3×. Although this work was developed for controlling reagent hydration in lateral-flow immunoassays, the concept is highly applicable for other μPAD detection motifs.

Surface Chemistry. Altering the surface chemistry of paper is an effective technique for controlling fluid flow,[108] improving color uniformity,[42] enhancing chemical stability,[109] and can even be applied to creating microfluidic valves.[110] Glavan et al.[66] infused cellulose with gas-phase fluoroalkyl silane to render the surface omniphobic. Channels were created using an *XY* crafting plotter. The authors took advantage of the folding properties of paper to create manual "fold" valves that reduced the rate of flow through them as long as the fold was perpendicular to the channel. When the folding angle was in excess of 90°, fluid flow ceased. Although probably not a solution for sequential assays with multiple steps where automation is desired, this type of valve gives highly reproducible performance, and the surface treatment of the device ensures compatibility with a much wider range of chemicals than many other paper-based technologies. Another limitation of this method was that the hydrophobicity of the channels dictated that flow was driven with an external pump, which ultimately limits their utility for power-free POC applications.

Once fully wetted, paper tends to lose much of its functionality for driving fluid transport. To address this limitation, Gong et al.[111] coupled a nanoporous membrane with ion concentration polarization to concentrate analytes and maintain fluidic transport even in fully saturated channels (Figure 4D). With ion concentration polarization, an electrochemical potential is applied at the interface of nanopores, creating a region of depleted ions which repels charged particles. Two versions of the device were developed: one in which the nanoporous membrane is separated from the paper device for sample concentration and another in which the membrane is embedded in the substrate for analyte transport. A fluorescent tracer was used to demonstrate that analyte could be transported several centimeters at a time and concentrated up to 40×. Application of ion concentration polarization to fluorescein isothiocyanate conjugated bovine serum albumin resulted in a 5× improvement in detection limit from 10 to 2 pmol/mL.

Electrode Incorporation. Printing conductive material for paper-based electrodes has been of interest for incorporating electrochemical, electrochemiluminescence, and photoelectrochemical detection.[45,112,113] Electrodes used in μPADs have typically been directly printed onto the device or coupled with external screen printed electrodes.[114] Screen-printed[115] (Figure 1C and 1I) or stencil-printed[116] carbon electrodes (SPCE) have been the most common fabrication technique for electrodes printed onto μPADs. Similar to wax-screen printing, ink or paste is pressed through a screen[115] or stencil[117] onto paper to form the desired electrode geometry and then cured. Santhiago et al.[118] used stencil-printing of carbon paste to demonstrate microelectrode fabrication with μPADs. The resulting microelectrodes were used individually, or in an array, for electrochemical detection. Santhiago et al.[119] also recently fabricated electrodes with pencil lead. Electrodes from pencil lead[112] or doped pencil lead[120] are easy to fabricate because they can be hand-drawn. Dossi et al.[121] made use of

dx.doi.org/10.1021/ac503968p | Anal. Chem. 2015, 87, 19−41

pencil lead doped with silver and silver chloride to draw stable reference electrodes when small amounts of chloride were present in the sample.

Besides carbon, other materials have recently been of interest for electrode fabrication. Screen-printed or stencil printed silver ink on paper has been used as connecting pads and for working, reference, or counter electrodes.[118,122] Lan et al.[116] presented a stable potential silver chloride reference electrode made of stencil printed silver ink. The electrochemical paper analytical device (ePAD) design separated the reference zone (reference electrode that was in contact with a reference solution in paper) from the sample zone (working and counter electrodes in contact with sample solution in paper) with a paper channel spacer that operated similar to a frit used in conventional silver chloride reference electrodes. Potentiometric ePAD devices were also developed using this stable reference electrode design.[123] Both the sample and reference zones contained stencil-printed silver electrodes but the sample zone incorporated an ion selective paper barrier over the reference electrode to create an ion selective electrode for detection. Gold nanoparticle (AuNP) ink electrodes were presented by Liana et al. and were applied to paper coated in nail polish to limit nanoparticle dispersion into the paper using a calligraphy pen.[124] The nanoparticles were made conductive using a camera flash sintering step to remove the organic stabilizing molecules. In another reported method, gold was electroplated onto SPCE by Cunningham et al.[125] Recently, Fosdick et al.[126] fabricated an ePAD device with carbon fiber and gold microwire electrodes.[126] An advantage of this fabrication technique is that aggressive electrode treatments or modifications that would contaminate or destroy the paper substrate can be done prior to electrode incorporation. The electrodes can also be made of a variety of prefabricated and highly conductive materials to tune detection and provide better electrochemical performance than carbon electrodes. Another method presented uses the porous and high surface area paper substrate itself as a basis for electrode fabrication. Ge et al.[127] created a unique working electrode by growing AuNPs that formed an interconnected layer on the surface of cellulose fibers. A SPCE was printed in contact with this network and acted as the connection to the potentiostat. Similar to AuNPs, nanoporous[128] or cuboid[129] silver nanoparticles (AgNPs), gold nanorods,[130] platinum nanospheres,[131] gold and manganese oxide nanoparticles,[131] and gold−palladium alloy nanoparticles have also been grown on cellulose fibers[132] and provided high conductance and surface area electrodes that could be tuned and modified for detection.

DETECTORS AND READOUT

One critical step for μPADs is the ability to quantify the analyte. The most common analytical detection technique for μPADs is colorimetry because analysis is relatively simple (i.e., color intensity is proportional to analyte concentration), and the technology is compatible with smartphone-based reporting systems. Moreover, the detectors (e.g., charge-coupled device (CCD), complementary metal-oxide sensor (CMOS), flatbed scanner) are relatively inexpensive and straightforward to operate with little to moderate training.[39,44,109,133−140] Additionally, detectors for colorimetric analysis can be made portable (vs traditional spectroscopy instrumentation) and have been demonstrated for on-site analysis[141,142] and classroom outreach.[134] Phone-based camera technology has progressed rapidly over the past several years; imaging and processing power have opened new doors for applying μPAD technology to analyte detection in many settings. The methods for quantitative readout discussed in this review include digital and cell phone cameras, smartphones, hand-held readers, and equipment-free methods.

Digital Cameras, Cell Phones, and Smartphones. The potential of telemedicine using μPADs was first demonstrated in 2008 for the determination of clinically relevant concentrations of glucose and protein in artificial urine.[143] Because of their market penetration and worldwide ubiquity, smartphones have created new opportunities for analysis in resource-limited settings either through on-site processing or remote data transfer to a centralized facility. Moreover, increased device data storage capacity enables information to be collected on-site and stored for transport to a central location without requiring sample transport. Because modern smartphones possess both a light source (LED flash) and a digital camera for detection, they are also amenable for tasks typically performed with more expensive spectrophotometers, fluorometers, or silicon photodetectors.[144]

Camera phones have recently been used for detection of phage and bacterial pathogens,[145−149] pharmaceuticals,[150,151] biomarkers,[152−156] explosives,[157] and toxic metals.[158,159] Although smartphones are superior to flatbed scanners in regards to portability, they suffer from changing ambient light conditions, rendering image intensities inconsistent. Recently, several groups addressed this problem by developing intensity-correction software for smartphones or by creating devices to physically block ambient light during image acquisition. In these examples, the phone's flash provides a (near) constant source of illumination by which to quantify assay results. For example, instead of using typical RGB intensity for quantification, Shen et al.[142] used chromaticity values to construct a reference chart with known color spaces to compensate for measurement errors due to ambient light. To overcome their ambient light problem, Thom and coworkers[160] modified a commercially available iPhone 4S case with a polyethylene tube designed to eliminate most incoming light and ensure appropriate focal length for every acquired image. In a similar fashion, the Erickson laboratory[150,153] has used a modified attachment to a smartphone that included an internal reference to minimize lighting effects for quantifying biomarkers in sweat, saliva, and blood.

Noninstrumented Analysis. Although much work has been done to reduce the cost and increase the portability of external readers, another goal (particularly for POC applications) is the development of accurate and easy-to-use devices that do not require external instrumentation. Quantitative or semiquantitative readouts are desired in many applications, particularly in the context of on-site diagnostics where treatment could be dictated by a simple "yes/no" or "normal/abnormal" response. The reader is encouraged to also review other works on the subject.[161,162]

One approach for noninstrumented analysis is use of a visual color intensity comparator built from a calibration that is integrated with the device. Calibration standards can be external (e.g., reference card) or on-device.[163,164] Weaver et al.[151] reported the development of an inexpensive "color bar code" test for rapid screening of potentially low-quality pharmaceutical drugs. The card was divided into 12 individual lanes, upon which the user rubbed the solid pharmaceutical across each lane and dipped the edge of the device containing each lane inlet into water. Each lane was sensitive to a specific

dx.doi.org/10.1021/ac503968p | Anal. Chem. 2015, 87, 19−41

analyte (e.g., ampicillin, amoxicillin, and rifampicin). A colored lane was indicative of a positive I.D., which was visually compared with an on-chip reference. Because of reaction variability and product stability, the authors specified an "optimal" time for reaction duration and analysis. Ambient conditions can have a tremendous impact on time-based analysis, thus many groups have attempted to design calibration standards for analysis when conditions are not optimal. For example, Zhu et al.[140] created a sensor for enzyme-based glucose measurements that was self-calibrating. The authors claimed that a simple tree-shaped branching structure with glucose standards spotted in each branch was sufficient for minimizing ambient temperature and relative humidity effects. In one notable study, instead of utilizing on-device calibrators, Pollock et al.[165] altered incubation times for analysis depending on differences in ambient temperature. Devices containing a test zone and positive and negative control zones were used to test 600 outpatients in Vietnam for HIV drug-induced liver injury. During the study devices were held in storage for up to 8 weeks, during which time storage temperatures varied from ~22−33 °C. Although device readouts were semiquantitative, the authors demonstrated that device operators (trained nurses) were 84% accurate through visual result assessments. This kind of field study demonstrates that visual assessment can be robust, although proper controls should be implemented for controlling ambient conditions.

In 1985, Zuk et al.[166] reported a method for measuring drugs in biological fluids by recording the total distance a colorimetric reaction product wicked along a porous channel. In this method, the total distance traveled was proportional to analyte concentration. The advantage this "distance-based" detection strategy has over previously reported methods is its potential for extracting more precise, quantitative information. In 2013, Cate et al.[167] revisited this detection motif by applying it to the measurement of heavy metals, small biological molecules, and reactive oxygen species.

Another strategy complementary to distance-based detection essentially involves breaking up the continuous flow path into discrete segments and then counting the number of segments that turn color. In this case, the number of segments tallied is proportional to analyte concentration. This semiquantitative approach has gained popularity due to its simplicity and applicability to a wide variety of chemistries. Since the first reported method for a paper-based digital readout,[168] groups have expanded this technique to include detection of hydrogen peroxide.[43,101] For example, Zhang et al.[43] measured H_2O_2 by essentially counting the number of successive detection zones that turned color after reaction with H_2O_2. A higher number of colored zones correlated with higher H_2O_2 concentration. In their chemical scheme, potassium iodide is reduced by H_2O_2 in an alkali environment to I_2, yielding a yellow-colored product. I_2 was then reoxidized by sodium hyposulfite, but when the concentration of sodium hyposulfite was limited, the yellow product of unreacted I_2 remains. All that is required for assay analysis is a timer or cellphone with timing functionality. This detection motif is especially suitable for remote environments because timers are simple to operate and are relatively inexpensive.

Quantifying analyte concentration using "time" is an alternative detection method where the time taken for signal to develop is the performance metric. Lewis et al.[101] developed a system for quantifying active enzyme concentrations with high sensitivity using a timed readout approach. A control region was implemented to account for temperature, pressure, relative humidity, and sample viscosity effects. For example, if the recorded ambient temperature during the assay were <15 °C, one additional minute was added to the vertical axis of the calibration curve to elicit the correct analyte measurement. Lewis et al.[100] further developed the time-readout motif with a phase-switching system in which poly(carbamate) oligomers undergo depolymerization in the presence of a target analyte, where the depolymerization rate is proportional to analyte concentration. The oligomers were initially hydrophobic but were converted to hydrophilic products, allowing flow through the device to a colored zone and indicating assay completion. The concentration of the target analyte was directly proportional to the time spent depolymerizing poly(carbamate) oligomers.

Hand-Held Devices. Bulky, benchtop instrumentation is typically too expensive for application in point-of-care settings. For instance, some μPAD technologies still use benchtop potentiostats, which can cost in excess of $10 000, while commercially available hand-held units cost >$1000. If μPAD technology is to have an impact in the medical or environmental community, the cost-structure system for detectors must be much lower. To this end, several groups have designed custom hand-held devices that are inexpensive and user-friendly for a variety of applications. Zhao et al.[169] built a custom low-cost eight-channel potentiostat for amperometric detection of glucose, lactate, and uric acid. The authors included a custom holder for a paper sensor with eight individual electrochemical wells. Though their design was based on previous work,[170] this system was the first of its kind to incorporate the detection of multiple electrochemical assays simultaneously from the same analyte sample. The current sensitivity ranged from tens of nA to over 1 mA, and the total unit cost was ~$90. More recently, the number of channels in a hand-held potentiostat was increased to 48.[171] Nemiroski et al.[172] created a hand-held potentiostat designed for resource-limited settings and capable of running a variety of electrochemical tests, on-board sample mixing, and wirelessly transmitting analytical data over voice through the cellphone audio jack. This data transfer was intended so that consumer phones built years ago would be compatible with their device. Other off-the-shelf hand-held devices have also been reported for measuring water contamination electrochemically[173] or explosives via fluorometry.[174]

APPLICATIONS: BIOMEDICAL

Colorimetric Detection: Enzymatic Methods. Glucose is one of the most important clinical analytes because of its role in diagnosing diabetes. Many colorimetric methods have been developed for glucose using either glucose oxidase (GOx) or GOx in combination with enzymes like horseradish peroxidase (HRP). For example, Zhu et. al used tree-shaped μPADS with 2,4,6-tribromo-3-hydroxy benzoic acid and 4-aminoantipyrine to detect glucose.[140] Interestingly, gelatin was used to protect enzyme activity during storage, which slowed the diffusion rate for optical color production. The detection limit and dynamic range were 0.8 mM and 2.4−11.4 mM, respectively, and the system was applied to determination in serum. In a second example, commercial assay kits were used for measuring protein and glucose in urine on a three-dimensional μPAD.[175] The standard concentration range detected by this device was 0.25−8 mg/dL for glucose and 5−20 mg/dL for protein. Another device was developed by Demirel et al.,[73] not only for the

dx.doi.org/10.1021/ac503968p | Anal. Chem. 2015, 87, 19−41

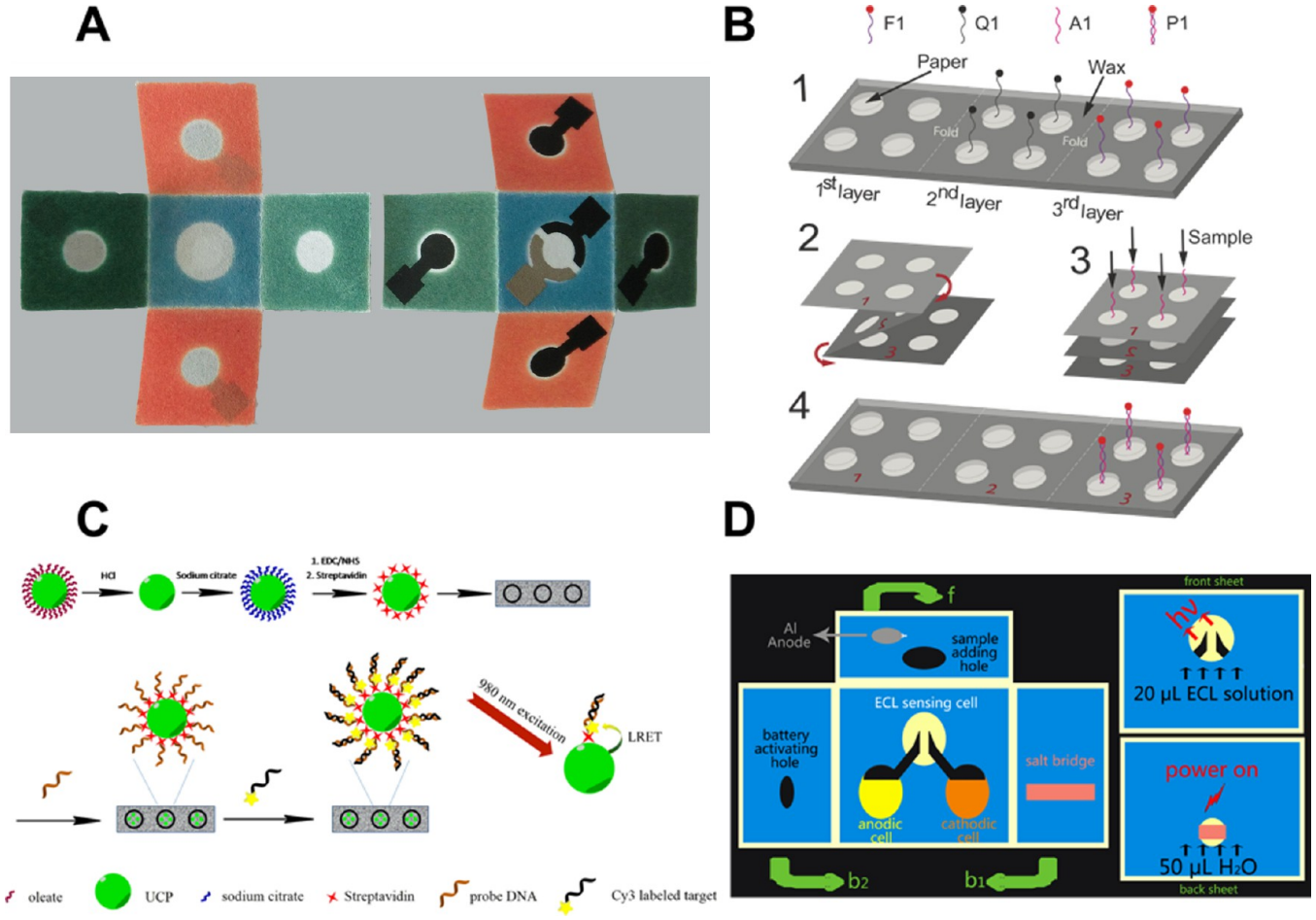

Figure 5. (A) Image of a PAD comprised of four working electrodes surrounding the counter and reference electrodes (center well). The top of the device is shown on the left, and the device flipped over (right). Reprinted with permission from ref 127. Copyright 2013 Wiley-VCH Verlag GmbH & Co. KGaA, Weinheim. (B) The overall reaction scheme is depicted in which upconverting phosphors undergo surface modification followed by hybridization with the target probe. Reprinted from ref 196. Copyright 2013 American Chemical Society. (C) A target probe is hybridized with a fluorophore-labeled probe to elicit a fluorescent signal. Reprinted from ref 197. Copyright 2014 American Chemical Society. (D) The working principle of the microfluidic origami PAD employing ECL detection. Reproduced from ref 211 with permission of The Royal Society of Chemistry.

enzymatic detection of glucose but also for albumin, uric acid, ALP, and alanine aminotransferase (ALT). Albumin was measured to quantify total protein based on the colorimetric reaction between albumin and tetrabromophenol blue, and ALP was enzymatically detected with nitro-blue tetrazolium and 5-bromo-4-chloro-3′-indolyphosphate. Uric acid and ALT were measured using commercial enzymatic assay kits applied to the μPAD. Moreover, Pollock et al.[176] fabricated 3D-μPADs for semiquantitative measurement of ALP and aspartate aminotransferase (AST) in blood or serum for liver function tests. Another device for glucose and ALP colorimetric measurement was demonstrated by Schilling et al.[91] To enhance portability, the device was completely sealed in plastic, which not only improved the mechanical stability but also reduced evaporation of the solution during transport in channels. The effect of paper substrate type on the intensity of color was studied for glucose detection; Whatman grade 1 filter paper was found to be most optimal.[67] Yetisen et al.[152] developed a smartphone algorithm to improve the portability of glucose detection using paper sensors. Their algorithm automatically accounted for the distance between the camera and the substrate, which dramatically increased the accuracy of the measurement. Chen et al.[177] used 3D channels to improve detection limits of glucose and uric acid by almost 1 order of magnitude versus other paper sensors using 2D channels.

Colorimetric Detection: Immunoassays. Detection of protein and DNA-based biomarkers is another promising area of research for point-of-care monitoring. Zhou et al.[178] used 3-aminopropyltriethoxysilane cross-linked with glutaraldehyde as a colorimetric reagent to detect H_2O_2. When H_2O_2 was present, the cross-linked APTES turned colorless after being degraded. This color change was used to detect the presence of prostate specific antigen (PSA). Anti-PSA immobilized on paper captured PSA and was labeled with GOx-modified gold nanorods. After addition of glucose, the amount of H_2O_2 generated correlated linearly with PSA concentration. Zhu et al.[108] modified the paper surface using zwitterionic poly(carboxybetaine) via surface-initiated atom transfer radical polymerization to improve device performance for both glucose enzymatic detection and immunoassays. Faster and more sensitive detection was achieved with modified paper relative to unmodified paper due to faster liquid transport in modified channels and decreased surface fouling. Guan et al.[109] studied the impact of polyvinylpyrrolidone, dextran, and glycerol additives on paper devices as well as freeze-drying to stabilize antibodies for immunoassays. All of the studied methods

dx.doi.org/10.1021/ac503968p | Anal. Chem. 2015, 87, 19−41

improved long-term stability and consistency of response but freeze-drying was the most successful. Bagherbaigi studied antibody immobilization strategies for cotton-based devices.[179] Three strategies were tested with gluteraldehye and adsorption methods working the best. Free-β-human chorionic gonadotropin was selectively detected using the method.

Colorimetric Detection: Other Applications. Other color-based detection methods have been used for paper devices, such as an innovative "color bar code" device developed by Lieberman's group[151] for testing active pharmaceutical ingredients in antituberculosis (TB) drugs. In a similar fashion, Koesdjojo et al.[180] developed a test for the counterfeit antimalarial drug artesunate. A paper-based sensor for measuring blood hemoglobin was also developed by Yang et al.[181] Drabkin reagent was added with blood to the device, leaving a concentration dependent color on the paper. Rohrman et al.[182] used μPADs for HIV DNA detection. Enzymatic amplification of the HIV DNA was successfully enhanced to 10 copies within 15 min by combining the enzyme storage, reaction component mixing, and recombinase polymerase amplification of HIV DNA steps on the paper.

Colorimetric Detection: Nanomaterials. Nanomaterials have found widespread use in cellulose and nitrocellulose-based paper platforms, primarily as detection reagents.[4,183] Nanoparticles (NPs) are popular because they tend to be more stable than organic molecules and typically have higher extinction coefficients, consequently leading to better sensitivity for target analytes (e.g., cancer antigens). A number of groups have developed nanoparticle-conjugated immunoassays that specifically take advantage of the high molar absorptivity of NPs to achieve low detection limits and high sensitivities. In these systems, detection is often performed visually, which is highly suitable for POC applications. To the present, modified nanoparticles have been used to measure cancer biomarkers,[57,184] antibodies,[184] bacteria,[185] proteins,[186] and infectious diseases.[148] Recently, Tsai et al.[148] demonstrated AuNPs as a detection reagent for TB DNA. AuNPs modified with single-stranded DNA (ssDNA) were hybridized with complementary dsDNA from TB positive patients. Upon DNA hybridization with AuNPs, a red to blue color change occurred. A mobile phone was utilized for measuring the intensity of the color change and data was transferred via cloud computing. With this method, *Mycobacterium tuberculosis* was measurable at concentrations as low as 2.6 nM and provided test results in less than an hour from extracted human DNA samples.

Some groups have devised other colorimetric detection methods that take advantage of the high surface area and catalytic functionality of nanoparticles but are easier to fabricate and have less detection variability. For example, Liu et al.[187] created a colorimetric immunosensor for carcinoembryonic antigen (CEA) using $ZnFe_2O_4$-carbon nanotubes, which exhibited peroxide-like catalytic behavior. Previously reported schemes used the reaction between H_2O_2 and HRP to measure analytes like glucose or bovine serum albumin in biological samples. However, natural enzymes like HRP suffer from poor stability, difficulty of preparation, and are highly influenced by ambient conditions.[188] The nanocomposites developed by Liu et al. were also generally less labile than previously reported methods. Secondary antibodies attached to the surface of metal-nanotubes were used to label the captured CEA for visual detection. A visible blue-green color change was apparent almost immediately after primary and secondary antibody binding due to a charge-transfer complex consisting of a free $^{\bullet}OH$ radical and 3,3′,5,5′-tetramethylbenzidine. CEA was measurable at concentrations ranging from 0.005 to 30 ng/mL, and the limit of detection was determined to be 2.6 pg/mL. Ge et al.[127] modified electrodes with AuNPs to create a multiplexed device consisting of one auxiliary electrode surrounded by four sample pads for detection of D-glutamate (Figure 5A). Layered AuNPs on the working electrode (grown from 3.5 nm seeds) created a high surface area to weight ratio (9.5 m^2/g) for electron transport through the porous matrix. The modified electrode's improved conductivity (1.15×10^{-5} Ω cm) versus a bare carbon electrode resulted in low nanomolar detection sensitivity of the amino acid target.

Electrochemical Detection. μPADs coupled with electrochemical detection (ePADs) offer a selective and sensitive platform for measuring biomarkers. Noiphung et al.[45] reported the electrochemical detection of glucose in whole blood using a reusable, external screen-printed carbon electrode (SPCE) modified with a mediator, Prussian Blue. Blood plasma carrying glucose was separated from whole blood into a detection region where it reacted with glucose oxidase to form hydrogen peroxide and detected electrochemically using amperometry. Glucose was also measured by Santhiago et al.[119] using GOx at graphite pencil electrodes with a *p*-aminophenylboronic acid mediator. Ge et al.[127] reported the sensitive detection of D-glutamic acid, a neurotransmitter associated with brain damage, using GNP coated cellulose fibers with electropolymerized molecular imprint polymer on the surface. When D-glutamic acid adsorbed to the electrode surface, a decrease in hexacyanoferrate oxidation was measured using differential pulse voltammetry (DPV) that correlated with D-glutamic acid concentration. This ePAD device was capable of sub-nanomolar detection and provided results comparable to HPLC testing of real human samples. Using pencil-drawn electrodes in a flow-through ePAD, Dossi et al.[112] successfully detected comigrating neurotransmitters paracetamol and ascorbic acid or dopamine and ascorbic acid using thin-layer chromatography. Simultaneous detection was possible using two working electrodes that first oxidized and then reduced the sample, resulting in combined electrochemical response for oxidation of DA and AA or PA and AA but only the reduction detection of PA or DA. The detection of DNA and protein was reported by Cunningham et al.[125] using conformational switching of an aptamer upon binding with the target analyte. The binding results in the location change of an electrochemical label (methylene blue) away from the gold electroplated SPCE surface, turning the signal "off," and providing detection limits in the low nanomolar range for both DNA and thrombin detection.

The electrochemical detection of low-abundant cancer biomarkers is of interest in early diagnostics and screening detection. Several papers have been published based on the sandwich assay technique of immunocapturing biomarkers and then immunotagging them with electrochemical signal enhancing tags. The papers discussed in this paragraph all provided detection results in good agreement with commercially available tests when human serum samples were tested. Nanoporous silver-coated cellulose fibers in contact with a SPCE were modified with antibodies specific to tumor markers CEA and alpha-fetoprotein.[128] Bound tumor markers were then selectively tagged with nanoporous gold-chitosan hybrids containing absorbed metal ions. These metal ions were then detected electrochemically using square wave voltammetry (SWV), and measured peak currents for each metal correlated

dx.doi.org/10.1021/ac503968p | *Anal. Chem.* 2015, 87, 19−41

linearly with biomarker concentration. The use of the high concentrations of metal (Pb(II) and Cd(II)) loaded onto tags allowed for multiplexed and simultaneous detection of analytes down to sub-pg/mL levels, which was significantly lower than previously reported methods. Using these same tags, Ma et al.[130] used differential pulse voltammetry to simultaneously detected immunocaptured CEA and cancer antigen 125 (CA125) on gold nanorod-coated cellulose fibers. Cuboid silver nanoparticle coated cellulose electrodes were also presented for the multiplexed detection of immunocaptured CA125 and carcinoma antigen 199 (CA199) using SWV to detect metal ion coated nanoporous silver-chitosan tags.[129] In a similar method Li et al. presented the multiplexed detection of immunocaptured and tagged CFA and AFP on polyaniline coated and interconnected gold nanoparticles immobilized on cellulose fibers.[189] The tags consisted of three-dimensional graphene oxide sheets with immobilized redox probes (methylene blue and carboxyl ferrocene) that were detected simultaneously using DPV with sub pg/mL detection limits of analytes. Gold and palladium alloy nanoparticle coated cellulose fibers immunocaptured CEA and were immunotagged with Au−Pt nanoparticles bound with GOx and methylene blue, resulting in the electrocatalytic detection of methylene blue and production of hydrogen peroxide in the presence of glucose.[132] Li et al.[131] detected prostate specific antigen (PSA) immunocaptured on nanostructured gold and manganese oxide coated cellulose fibers and immunotagged with carbon nanospheres bound with glucose oxidase. The glucose oxidase reacted with glucose to produce hydrogen peroxide that was electrocatalytically detected using DPV. A graphene oxide coated (to accelerate electron transfer) SPCE with immobilized antibodies was used to capture AFP, CEA, CA125, and carbohydrate antigen 153 (CA153) each on individual electrodes in a multiplexed ePAD device.[57] Silicon dioxide nanoparticles with bound HRP were used to immunotag targeted cancer biomarkers and react with hydrogen peroxide and *O*-phenylenediamine (*o*-PD) to produce 2,2′-diaminoazobenzene which was detected using DPV.

Cultured cancer cells are also of interest and can be used to monitor cellular activity and screen for potential therapy drugs. Su et al. and Liu et al. reported the culture of cancer cells in 3D paper-based devices capable of monitoring cellular apoptosis, glycan production, and hydrogen peroxide release in anticancer drug screening.[190−192] AuNP-coated cellulose in contact with a SPCE, aptamer captured cancer cells on the electrode surface were labeled with HRP-conjugated aptamers that catalyzed oxidation of o-PD by H_2O_2 to produce DPV detectable 2,2′-diaminoazobenzene.[190] Cellular apoptosis with leukemia drug application resulted in increased signal due to the increase in concentration of HRP-annexin-V aptamer tag, which specifically binds to apoptotic cells. Using this same detection scheme with glycan aptamer-HRP tags, glycan expression that changed due to drug application could also be monitored.[192] Pt nanosphere coated fibers detected the nonenzymatic release of hydrogen peroxide from living cells and also due to drug induced apoptosis.[191] Another 3D ePAD cell culture device was developed by Shi et al.[193] using carbon-paper electrodes modified with carbon nanotube, graphene oxide, and manganese oxide aerogel for the detection of H_2O_2.

Fluorescence. Several examples of fluorescence-based μPADs have been demonstrated.[62,174] Fluorophores are attractive because they are sensitive; however, one drawback is that paper whitening additives can increase background fluorescence. Within the last 2 years, examples of fluorophore-based sensors have been applied to the detection of bacteria,[194] biological proteins,[53] and cancer biomarkers.[195] Only recently has DNA detection been extended to paper substrates. One possible reason is because paper-based techniques are not capable of the sub-nanomolar detection sensitivities required for typical DNA-detection applications. Recently, Scida et al.[196] introduced a competitive hybridization assay to detect fluorophore-labeled ssDNA using capture ssDNA and quencher-labeled ssDNA, and medically relevant detection limits of less than 5 nM (% relative standard deviation <3%) were obtained. The μPAD used for analysis contained four-layers and four independent testing zones in three of the layers. As depicted in Figure 5B, quencher and fluorescent-labeled ssDNA were applied to detection zones in separate device layers but were brought into contact after the device was folded. In a separate case, both quencher and fluorophore-labeled ssDNA were premixed. Clamps were used to close the device. Target analyte, upon addition, displaces a strand of quencher-labeled ssDNA from fluorophore-labeled ssDNA because it has eight more matching bases than the quencher, producing a fluorescent signal that was linearly proportional to target DNA concentration. The signal was measured as analyte solution moved to the third layer of the device. It was found that allowing hybridization of the quencher and fluorophore prior to incorporation into the device proved to be superior to drying them separately on the substrate (14% vs 3% % RSD, respectively), possibly due to nonspecific absorbance of ssDNA on paper.

Chemiluminescence. Chemiluminescence-based sensors measure light intensity generated by a chemical reaction. Reagents for chemiluminescence (CL) are typically inexpensive, and the measurement is highly sensitive, making it very attractive for low-cost high sensitivity assays. Photochemiluminescence (PL), a subset technique of chemiluminescence, was demonstrated with μPADs by Zhou et al.[197] for in-field and POC application using luminescence resonant energy transfer associated with upconverting phosphors. Green-emitting upconverting phosphors were functionalized with streptavidin and immobilized on paper before biotinylation occurred with single-stranded oligonucleotide probes. The reaction sequence is depicted in Figure 5C. A biotinylated DNA target probe (SMN1) containing Cy3-labeled oliqonucleotides was hybridized with the phosphor-strep complex. Luminescence emission occurred upon excitation of the conjugate probe at 980 nm and was analyzed with an epifluorescence microscope. Hybridization was complete in ∼2 min with a detection limit of the target probe of ∼30 fmol. Wang et al.[198] also developed a μPAD for measuring DNA hybridization using photoelectrochemiluminescnce (PEL) but integrated Au-paper electrodes to obtain ∼femtomolar detection limits. The authors integrated a novel, paper-based supercapacitor to amplify the PEL signal by allowing it to continually charge until it was automatically shorted after a fixed period, releasing an amplified current to a terminal multimeter. Developing an automated method for timing the charging period was crucial, so the authors created a fluidic-delay switch by repeatedly dropping and drying a 1 M NaCl solution containing AuNP-modified multiwall carbon nanotubes to the end of a hydrophilic strip 26 mm in length. The end of the channel also contained a conductive pad, triggering an electrical switch once reached by wicking fluid.

dx.doi.org/10.1021/ac503968p | *Anal. Chem.* 2015, 87, 19−41

Electrochemiluminescence. Electrogenerated chemiluminescence (ECL) is an alternative for μPAD analysis that uses electrochemical reactions to generate luminescence.[144,199,200] The advantages ECL confers versus CL and PL are multifold: background optical signals are low, controlling electrode potential is easier than controlling reagent addition at specific times, and selectivity is enhanced by controlling electrode potential.[201−206] Much of the recent work regarding the integration of ECL with paper devices involves the development of new approaches to consolidate power and measurement tools.[198,207]

In their seminal work, Delaney et al.[199] used a mobile phone camera for ECL detection. They recently expanded this work to address a critical challenge facing paper-based ECL detection, namely, how to apply the potential to paper-based electrodes without relying on expensive potentiostats.[158] The authors address this limitation by driving electrode potential from the audio socket of a camera phone to initiate the electrochemical reaction. The maximum output voltage was 1.77 V. Phone software and a custom-built app gave the user control of audio functionality such as the frequency, amplitude, and duration of square-wave pulses sent to the working electrode. The ECL signal intensity was captured using individual frames of the phone's video feature at 30 fps (320 × 240 pixel resolution) with red-channel intensity being proportional to analyte concentration. The group demonstrated a working device with the popular ECL coreactant, 2-(dibutylamino)-ethanol, as well as L-proline.[208] Limits of quantification achieved for both analytes were 100 μM with the linear range for L-proline extended to 10 mM.

Other efforts have been made to remove the bulk and expense incurred with electrochemical workstations by integrating a power source directly onto the sensor.[209,210] Zhang et al.[211] recently attempted to improve on-device power by developing an environmentally friendly battery with a relatively simple circuit which is activated with the addition of water (Figure 5D). The authors employed an origami folding technique to keep features aligned during the fabrication process and to reduce fabrication complexity. Noble metals were not included as part of the primary battery (C|$FeCl_3$|NaCl|$AlCl_3$|Al), reducing material costs. Moreover, Fe(III) is more stable than the typical Ag(I) so the device can be stored without use for longer periods of time. The open circuit voltage was reportedly stable during use for at least 250 s and did not deviate significantly when stored for 15 consecutive days. The best power density achieved was 0.52 ± 0.026 mJ cm^{-2} (V_{oc} = 1.3 V, I_{sc} = 0.4 ± 0.02 mA cm_{-2}). Luminol, $Ru(bpy)_3^{2+}$, and glucose detection were demonstrated with a linear detectable range for glucose from 10 nM to 10 μM (LOD = 1.7 nM).

Other Sensor Types. Other sensor motifs have recently been demonstrated for biomedical applications. Examples requiring instruments for detection include calorimetry[212] and light-reflectance.[33] Surface-enhanced Raman scattering has also been demonstrated for medical and environmental applications.[213,214] In 2014, digital microfluidics (DMF) on paper was demonstrated for the first time to measure rubella in an IgG sandwich ELISA.[215] DMF is a well-studied microfluidic technology[216] but had not been applied to paper microfluidics until recently. The DMF technology manipulates small liquid droplets (nanoliter to microliter) on an array of electrodes using electric fields. By controlling the applied fields in the array, functions such as droplet merging, splitting, mixing, and directional flow are feasible. In the work, DMF devices were formed by printing arrays of silver ink on filter paper; for operation, droplets were sandwiched between two printed layers. Droplet volumes between 0.4 and 0.8 μL were used for study, and contrary to previously established techniques for fabricating DMF devices, the paper sensors in the study cost less than $0.05 each. A major advantage of DMF is that controlling multistep sequences is simple; a calibration curve requiring 63 discrete steps was demonstrated for HRP mixed with luminol/H_2O_2 (Figure 6). The passive nature of paper typically limits the number of fluidic manipulations possible.

APPLICATIONS: ENVIRONMENTAL

Paper-based approaches for environmental monitoring are attractive because accurate, low-cost monitoring is pivotal for environmental applications where routine testing is performed, such as for the analysis of river/soil contamination, occupational exposures, or air pollution. Prior to 2013, noted papers were published on the detection of metal ions, chemical warfare agents, and reactive oxygen species using colorimetric,[88,135,217−220] electrochemical,[117] fluorescent,[221] and other analytical approaches.[222] Samples were sourced from water, soil, and air (i.e., particulate matter, polycyclic aromatic hydrocarbons (PAHs)).

Colorimetric Sensing. Many colorimetric μPADs have been developed for metal detection because of their known toxicity. Environmental metal contamination is common in three sources, air (aerosols), water, and soil. One of the first examples of μPAD-based quantification of metals was a sensor comprised of four detection zones for simultaneously measuring Fe, Cu, and Ni from combustion ash.[88] Aerosolized metals were collected on filters and transferred to a μPAD that had been treated with chromogenic reagents. Detection limits ranged from 1 to 1.5 μg (total mass) for each metal analyte. Detection on paper has recently been applied to measuring other metals.[85,137,223−225] Environmental measurement of Cu is important because it is used in a variety of applications, can easily find its way into water sources, and is toxic at elevated levels.[226,227] Different strategies for measuring Cu with μPADs have been reported. Jayawardane et al.[223] created a multilayer disposable device incorporating a polymer exclusion membrane modified with 1-(2′-pyridylazo)-2-naphthol as the colorimetric reagent for Cu detection (Figure 7A). To encourage analyte preconcentration, the authors stacked filters, with each successive layer allowing 9.6 μL more eluent to be flushed through the device and onto the detection membrane. Samples from hot tap water and mine leach residue were evaluated with the device, and detection and quantification limits of 60 and 210 μg/L, respectively, were reported. More recently, Li et al.[228] presented a device for measuring Cu in water and achieved detection limits approximately 10^4-fold lower using TiO_2 nanoparticles that functioned as a combined adsorbent, photocatalyst, and colorimetric reagent. Nanoparticles have also been used for metal detection with μPADs.[229] Chen et al.[230] demonstrated a surface plasmon coupling strategy for measuring Hg(II) using thymine-Hg(II)-thymine coordination chemistry to reach 50 nM detection sensitivities from spiked pond and river water. Surface plasmon coupling occurs when label-free oligonucleotide sequences, attached to the AuNP surface, possessed thymine-thymine mismatches. When introduced into an aqueous solution containing Hg(II), ssDNA on the particle surface underwent conformational changes, inducing AuNP aggregation and a subsequent color change.

dx.doi.org/10.1021/ac503968p | Anal. Chem. 2015, 87, 19−41

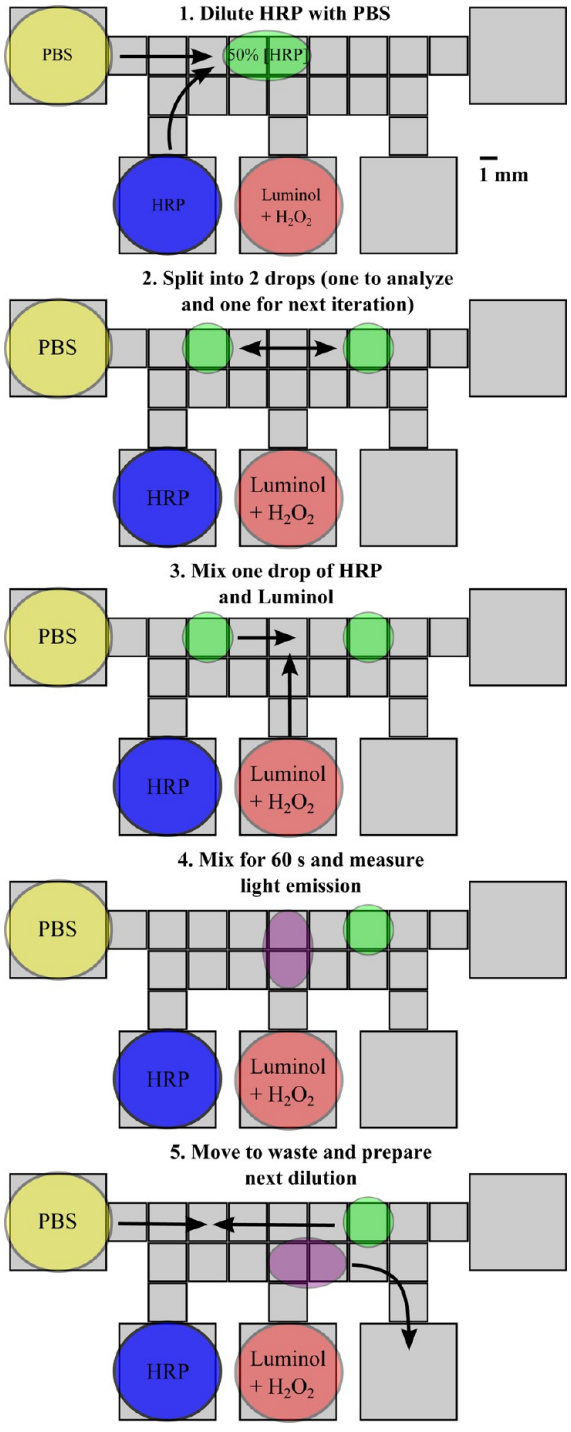

Figure 6. Schematic depicting the individual steps of a chemiluminescence assay for HRP with luminol/H_2O_2. HRP is first serial diluted before being mixed for 60 s with luminol/H_2O_2. The initial splitting occurs for subsequent dilutions. Reprinted with permission from ref 215. Copyright 2014 Wiley-VCH Verlag GmbH & Co. KGaA, Weinheim.

To reduce the cost of analysis, the authors utilized smartphone and cloud-computing technology for a quantitative readout.

μPADs have also been developed for nonmetal environmental analytes.[164,231−233] For example, a paper sensor to test for the presence of nitrite and nitrate in drinking water was presented by Jayawardane et al.[234] which, under optimal conditions, allowed the user to measure concentrations as low as 1 and 19 μM for nitrite and nitrate, respectively. The device contained two individual colorimetric detection zones for measuring nitrite (zone 1) and combined nitrate and nitrite (zone 2). The reported detection limits were well below the maximum contaminant levels (71.4 and 714.3 μM for nitrite and nitrate, respectively) stipulated by the U.S. Environmental Protection Agency. Pesenti et al.[235] reported a μPAD design for detecting 2,4,6-trinitrotoluene (TNT), 1,3,5-trinitrobenzene (TNB), and 2,4,6-trinitrophenyl-methylnitramine (tetryl) in explosive residue (Figure 7B). With their method, potassium peroxide acts as a complexing reagent, and analyte transfer occurs via a swab or by wiping a contaminated surface with the device. Violet color formation occurs via the Janowski reaction when hydroxide or methoxide ions are mixed with trinitro aromatics.[236] Detection limits reported were TNT (12.5 ± 2.0 ng), TNB (7.5 ± 1.0 ng), and tetryl (15.0 ± 2.0 ng) with extraction efficiencies over 96%. Quantification of other compounds found in improvised explosives such as RDX, urea nitrate, and TATP have also been reported.[237] Dungchai et al.[238] developed a AgNP method for measuring reduced glutathione, an endogenous antioxidant and indicator of cellular oxidative stress. Dithiothreitol is traditionally used for determining reactive oxygen species, but it is not endogenously produced in biological systems, making it an indirect measurement system. The authors used two different paper-based methods for detection, one based on color change and the second based on the length of a colored formation complex.

Culture plates are a standardized method for counting bacteria; unfortunately, this method can be tedious, time-consuming, and expensive. Additionally, large volumes of media are consumed during the process. Bisha et al.[239] studied bacteria in agricultural runoff using a colorimetric spot test. An attempt by Deiss et al.[240] was made to replace the traditional (plastic) Petri dish method with a sealed paper-based device for detecting bacteria, primarily in areas remote from centralized facilities. This portable culture device was capable of determining antibiotic susceptibility of several strains of *E. coli* and *Salmonella typhimurium*. The device is essentially the Kirby-Bauer antibiotic susceptibility test applied to paper.[241] The diffusion of a blue dye (PrestoBlue) indicative of bacterial antibiotic susceptibility (e.g., tetracycline, ampicillin, or kanamycin) was measured radially from a circular zone of applied antibiotic. Upon entering living cells, the dye encountered a reducing cytosolic environment and turned pinkish-red, which is indicative of bacteria resistant to a specific antibiotic. A larger radius of blue dye was correlated with greater bacterial susceptibility. Results for ampicillin resistance were compared to the traditional method of counting colony forming units on agar plates (Figure 7C). Ma et al.[47] created an immunoassay screening device for *E. coli* in drinking water. In a paper well, capture antibodies were immobilized by adsorbing to the substrate. Sequential introduction of *E. coli* and AuNP-labeled secondary antibodies formed an antibody-antigen-antibody complex visible to the unaided eye only after Ag was added to the system. AuNPs can catalyze the reduction of Ag ions, which deposit around the AuNPs, forming a visible gray-black product from strong light scatter. A darker spot signified a higher concentration of colony forming units. With their method, the authors were able to confirm the presence of *E. coli* at 57 CFU/mL and above; comparison studies with conventional ELISA were not statistically different.

Nanoparticles have also been used as colorimetric reagents to detect environmental pollutants. Sun et al.[242] developed a

dx.doi.org/10.1021/ac503968p | *Anal. Chem.* 2015, 87, 19−41

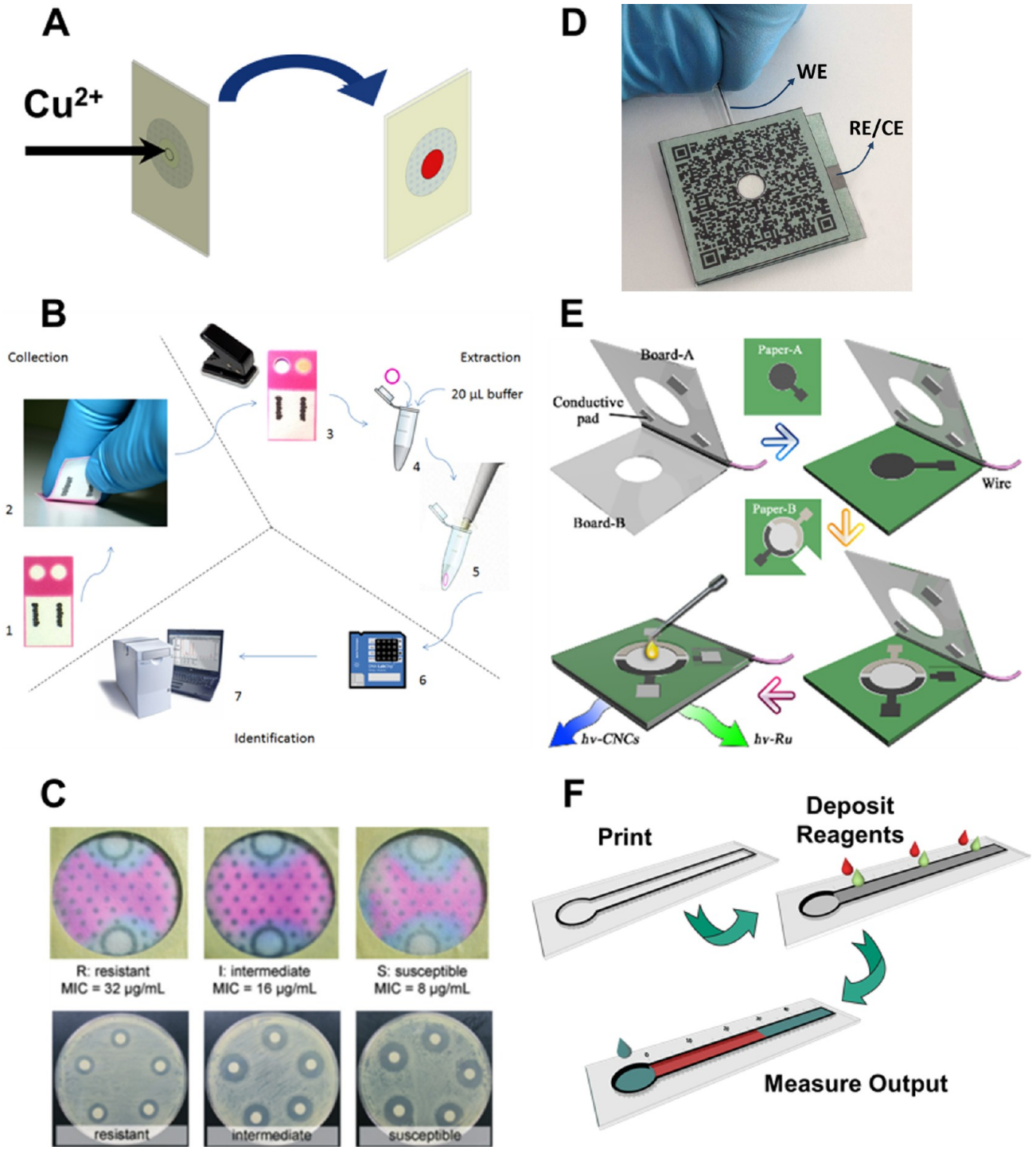

Figure 7. Environmental sensing approaches. (A) Cu^{2+} ions are selectively determined after passing through a polymer exclusion membrane with PAN as the immobilizing agent. Reprinted with permission from ref 223. Copyright 2013, with permission from Elsevier. (B) TNT is measured from a sample surface by swabbing with a paper device containing potassium peroxide. Reprinted from ref 235. Copyright 2014 American Chemical Society. (C) Strains of *E. coli* with light, intermediate, and heavy ampicillin resistance are characterized with a paper sensor. Reproduced from ref 240 with permission of The Royal Society of Chemistry. Copyright 2014 The Royal Society of Chemistry. (D) Pencil graphite was used as the working and reference electrodes to measure *p*-nitrophenol. Reprinted with permission from ref 113. Copyright 2014, with permission from Elsevier. (E) Schematic representation of an ECL μPAD. Reprinted with permission from ref 250. Copyright 2013, with permission from Elsevier. (F) Schematic diagram of distance-based detection for Ni^{2+}. Reproduced with permission from ref 167. Copyright 2013, by permission of the Royal Society of Chemistry.

photoelectrochemical immunosensor for detecting pentachlorophenol with polypyrrole-functionalized ZnO nanospheres by molecular imprinting. In their work, a layer of AuNPs was deposited on the paper surface, followed by ZnO and electropolymerization of polypyrrole. The group was able to measure pentachlorophenol as low as 4 pg/mL with a linear range of 0.01−100 ng/mL. Photoelectrochemical immunosensing of pentachlorophenol was demonstrated by Kang et al.[243] in

dx.doi.org/10.1021/ac503968p | *Anal. Chem.* 2015, 87, 19−41

2010. While successful, their method required antibodies, which increase cost and lack stability in harsh environments. The biomimetic receptor system utilized by Sun et al. was more chemically and physically robust than traditional antibodies.

Electrochemical Sensing. In some instances, the sensitivity and selectivity afforded by colorimetric detection falls short for environmentally relevant applications. For instance, current U.S. EPA regulations for Cd in drinking water are 5 ppb,[244] well below detection limits for existing colorimetric methods. Additionally, colorimetry can suffer from poor selectivity. Electrochemistry is an attractive alternative because detection limits are lower and sensitivity is higher. The first demonstration of electrochemistry on paper was in 2009.[115] Since then, a host of new electrochemical methods and applications have been developed coupling the advantages of paper substrates with electrochemistry.[72] One of the most recent applications is for the measurement of *p*-nitrophenol (pNp), a compound toxic to humans that can enter the water supply as a result of runoff from wastewater and agriculture. Ingestion of pNp can cause fever, headaches, respiratory congestion, and even death in severe instances.[245] Santhiago et al.[113] created a multilayer device using the graphite from a pencil as the working electrode (Figure 7D). The pencil graphite improves the system performance because it is highly conductive, widely available, and relatively inexpensive. Experiments were conducted using two different grades of pencil, H (less carbon = softer) and 6B (more carbon = stiffer). The group discovered that the graphite composition of grade H pencils had lower background currents and ΔEp. Concentrations of pNp from 10 to 200 μM (linear range) or as low as ~1 μM (LOD) were quantifiable. Because the sensing technique had application for field-testing, the authors integrated a quick response code (or QR code) feedback system that was affixed beside each assay on the paper support. The implementation of the QR code enabled a user to quickly gather and store pertinent information about each assay on a portable electronic device.

Ion-selective potentiometric sensing has also been used with μPADs because, in addition to other properties, paper is a suitable filtering agent for large particles. In 2013, Cui et al.[246] developed a paper sensor comprised of solid-contact ion sensing and reference electrodes to determine the concentration of K^+ ions in samples absorbed into a paper substrate. In their work, the sensing electrode was fabricated using poly(3,4-ethylenedioxythiophene) and plasticized PVC containing the K(I)-specific valinomycin ionophore. Detection limits were subsequently improved by Mensah et al.[247] by impregnating the paper with single-walled carbon nanotubes.

Luminescence Detection. A paper-sensor based on fluorescence-quenching of pyrene was developed by Taudte et al.[174] for detecting explosives. Although pyrene is an excellent fluorophore, its low-solubility in polar solvents prompted the authors to use 80:20 MeOH−H_2O for pyrene dissolution, and the wax boundaries were able to contain this solution. A total of 10 explosives were tested for fluorescence quenching under UV radiation; detection limits ranged from 100 to 600 ppm. To enhance the portability of the sensor, the authors designed and built a portable instrument for detection that incorporated a 365 nm UV LED for excitation of pyrene and a photodiode to capture emitted light at 500 nm. The sensor also contained a calibration procedure for when new paper-sensors were used.

Electrochemiluminescent (ECL) has also been used for environmental measurements. One of the first groups to implement ECL detection using μPADs was Delaney et al. for detection of 2-(dibutylamino)-ethanol (DBAE) and NADH.[199] Paper-based ECL has also been applied for detecting explosives[248] and genotoxic compounds.[249] Zhang et al.[250] recently applied paper-based ECL for detecting Pb(II) and Hg(II) from samples of lake water and human serum (Figure 7E). The ECL signal was generated from carbon nanocrystal-capped silica nanoparticles (for Pb(II)) and from $Ru(bpy)_3^{2+}$-AuNP aggregates (for Hg(II)). In this case, fluorescent carbon nanocrystals were utilized due to their low toxicity and abundance of −COOH groups at surfaces. Two different ECL labels were used so both metals could be measured simultaneously at different potentials from a single sample. In the presence of analyte, DNA bound to functionalized μPADs underwent a conformational change, leading to an increase in ECL signal intensity. Limits of detection for Pb(II) and Hg(II) were 10 pM and 0.2 nM, respectively.

Noninstrumented Detection. One of the limitations of any of the previously discussed sensing motifs is the need for peripheral equipment for analysis. The reagent costs are low, however instrumentation costs remain high. In 2013 Cate et al.[167] repurposed a noninstrumented technique for "distance-based detection" of heavy metals, small molecules, and reactive oxygen species. In their approach, colorimetric reagents designed to precipitate upon complexation with an analyte were patterned along the flow path of a paper channel approximately 2 mm wide. The analyte is consumed as fluid flow progresses along the device until no analyte remains, leaving behind a band of color in which the band length is proportional to analyte concentration (Figure 7F).

APPLICATIONS: FOOD AND BEVERAGE CONTAMINATION

Paper-based devices have been proposed as a preventative detection method to provide simple, low-cost, and on-site detection of foodborne contaminants.[232] μPAD devices developed for bacteria detection in food have relied primarily on enzymatic activity or immunoassays for detection. Colorimetric detection based on the reaction of enzymes produced by bacteria with a chromogenic substrate has been demonstrated in μPADs.[232,239,251] Because detection generally requires bacterial growth for enzyme production, this method has the advantage of being able to detect live bacteria. Jokerst et al. sampled bacteria from foods using a swab sampling technique.[251] The resulting swab sample was cultured in media before being added to a paper-based well device impregnated with chromogenic substrate. Ready-to-eat meat samples inoculated with *Listeria monocytogenes*, *E. coli* O157:H7, and *Salmonella typhimurium* were successfully detected. Detection limits as low as 10^1 CFU/mL were achieved in 12 h or less, which is significantly less time than the gold standard culture methods. Another method presented by Park et al. used antibody conjugated polystyrene nanoparticles for *Salmonella typhimurium* detection.[147] Instead of colorimetric detection, however, portable cell phone detection was used to measure light scattering intensity. Lysed bacteria added to a paper-based device flowed over preloaded antibody conjugated polystyrene beads. The presence of the target antigen caused immmunoagglutination and increased measured light scattering. While no real samples were tested, this method could be used for both food and water contamination detection. Currently the only

dx.doi.org/10.1021/ac503968p | *Anal. Chem.* 2015, 87, 19−41

example of paper-based electrochemical detection of bacteria was presented by Wang et al.[252] The working electrode consisted of antibody-conjugated AuNPs on a reduced graphene oxide paper-based electrode. The antibodies on the electrode surface captured target bacteria, which caused a measured change in impedance that correlated linearly with bacteria concentration. This method successfully detected *E. coli* O157:H7 from both ground beef (LOD of 1.5×10^4 CFU/mL) and cucumber (LOD of 1.5×10^3 CFU/mL) food samples.

Chemical contaminants such as heavy metals and pesticides have been detected in food and beverage samples using μPADs. Pb and Cd were detected electrochemically using square wave anodic stripping voltammetry (SWASV) by Shi et al. in soda water beverages.[253] In their approach, solution flowed through paper across the surface of screen-printed carbon electrodes. Chemiluminescence detection combined with paper chromatography was used by Liu et al. to detect the pesticide contaminant, dichlorvos (DDV), eluted from the skin of vegetables.[254] Ascending paper chromatography was first used to filter and separate DDV from other interfering species into a detection zone. The resulting purified zone was cut out and placed into a paper-based device. When hydrogen peroxide and luminol were added to the detection zone, the produced CL correlated linearly with DDV concentration. A μPAD developed for detection of genotoxicity in food samples was also reported by Mani et al. using ECL detection.[249] Paper-based wells with SPCEs contained enzymes that reacted with test compounds to produce reactive metabolites. These metabolites damaged bound DNA, which increased the reactivity of DNA with a Ru(III) substrate. When a voltage was applied to the cell the resulting reactivity produced ECL light that increased with greater DNA damage, correlating with genotoxicity of a sample.

CONCLUSIONS AND FUTURE DIRECTIONS

Since Martinez et al. published their use of photoresist to pattern paper for microfluidic assays there has been an explosion in the interest around the topic with research groups from around the world taking active part in the development cycle.[5] While paper-based analytical devices are not new, their use has primarily been limited to one-dimensional methods like litmus paper and lateral flow immunoassays. μPADs have challenged this paradigm resulting in increasingly complex devices and analytical assays. In particular, the development of complicated 3D devices that carry out multiple chemical reactions in a simple to use format that does not require any external reading equipment is an example of the potential of this field for solving complex problems.[103] More and more complicated chemistry and biology are also being demonstrated on paper including development of PCR-based assays[182] and cell culture.[145] Finally, μPADs are being developed for a diverse set of applications ranging from the original clinical diagnostic applications to environmental applications.[6] While the field of paper-based sensors has expanded rapidly, there are many areas that still need to be addressed. For example, most groups use a single form of filter paper, and while successful, it points to the potential for exploring alternative porous materials. Alternative porous materials compatible with organic solvents could offer many opportunities for continued expansion of the field as well as revisiting the fundamental materials chemistry of these devices.

In the end, the success or failure of μPADs will likely be determined by their use outside of academic research laboratories, much like traditional microfluidic devices. While significant attention has rightfully been placed on the potential for improved clinical diagnostics, there remain many other areas for future expansion. Particularly exciting is the potential for application of μPADs for large epidemiology studies where analytical measurements have traditionally been a cost limiting factor. In a similar fashion, the low cost and ease of use may open the door to widespread analytical measurements thereby enabling the growing field of citizen science. In a fashion similar to precipitation monitoring in the United States by everyday citizens,[255] μPADs may open the door to widespread environmental monitoring with spatial resolution that has never been achieved in previous studies.[256] Achieving these end points, however, requires continued development of the basic chemistry of sensing with μPADs.

AUTHOR INFORMATION

Corresponding Author

*E-mail: Chuck.Henry@colostate.edu. Phone: +1-970-491-2852.

Author Contributions

All authors contributed to the writing of the manuscript and have approved the final version.

Notes

The authors declare no competing financial interest.

Biographies

David M. Cate received his B.S. in Bioengineering from the University of Washington in 2009. He is currently a graduate student in the Department of Biomedical Engineering at Colorado State University. His research focuses on the development of low-cost paper sensors for personal exposure monitoring of metal particulates in air pollution.

Jaclyn A. Adkins received her B.S. in Chemistry from Northwest Missouri State University in 2010. Currently, she is a graduate student in the Chemistry Department at Colorado State University. Her research focuses on the detection of bacteria with paper-based devices and the development of electrochemical paper-based analytical devices.

Jaruwan Mettakoonpitak received her B.Sc. and M.Sc. in Chemistry from Mahidol University, Thailand. Currently, she is a graduate student in the Chemistry Department at Colorado State University. She is currently developing new separation techniques for application with paper-based devices.

Charles S. Henry received his Ph.D. in Analytical Chemistry from the University of Arkansas followed by postdoctoral studies as an NIH postdoctoral fellow at the University of Kansas. He started his academic career at Mississippi State University before moving to Colorado State University in 2002. He is currently a full professor and department chair of Chemistry at Colorado State University and also serves as a faculty member in Chemical & Biological Engineering and Biomedical Engineering.

ACKNOWLEDGMENTS

This work was supported by MAP-ERC (Grant T42OH009229) and the National Institute for Occupational Safety and Health (Grant R21OH010050).

REFERENCES

(1) Davy, J. *Phil. Trans.* **1812**, 144.
(2) West, P. W. *Ind. Eng. Chem. Anal. Ed.* **1945**, *17*, 740−741.

(3) Consden, R.; Gordon, A. H.; Martin, A. J. P. *Biochem. J.* **1944**, *38*, 224−232.
(4) Posthuma-Trumpie, G. A.; Korf, J.; van Amerongen, A. *Anal. Bioanal. Chem.* **2009**, *393*, 569−582.
(5) Martinez, A. W.; Phillips, S. T.; Butte, M. J.; Whitesides, G. M. *Angew. Chem. Int. Ed.* **2007**, *46*, 1318−1320.
(6) Yetisen, A. K.; Akram, M. S.; Lowe, C. R. *Lab Chip* **2013**, *13*, 2210−2251.
(7) Tobjörk, D.; Österbacka, R. *Adv. Mater.* **2011**, *23*, 1935−1961.
(8) Nguyen, T. H.; Fraiwan, A.; Choi, S. *Biosens. Bioelectron.* **2014**, *54*, 640−649.
(9) Coltro, W. K. T.; de Jesus, D. P.; da Silva, J. A. F.; do Lago, C. L.; Carrilho, E. *Electrophoresis* **2010**, *31*, 2487−2498.
(10) Ballerini, D. R.; Li, X.; Shen, W. *Microfluid. Nanofluid.* **2012**, *13*, 769−787.
(11) Liana, D. D.; Raguse, B.; Gooding, J. J.; Chow, E. *Sensors* **2012**, *12*, 11505−11526.
(12) Hu, J.; Wang, S.; Wang, L.; Li, F.; Pingguan-Murphy, B.; Lu, T. J.; Xu, F. *Biosens. Bioelectron.* **2014**, *54*, 585−597.
(13) Kauffman, P.; Fu, E.; Lutz, B.; Yager, P. *Lab Chip* **2010**, *10*, 2614−2617.
(14) Fu, E.; Ramsey, S. A.; Kauffman, P.; Lutz, B.; Yager, P. *Microfluid. Nanofluid.* **2011**, *10*, 29−35.
(15) Osborn, J. L.; Lutz, B.; Fu, E.; Kauffman, P.; Stevens, D. Y.; Yager, P. *Lab Chip* **2010**, *10*, 2659−2665.
(16) Kim, J.; Kim, H.-Y. *J. Mech. Sci. Technol.* **2012**, *26*, 3795−3801.
(17) Xu, Y.; Enomae, T. *RSC Adv.* **2014**, *4*, 12867−12872.
(18) Ponomarenko, A.; Quéré, D.; Clanet, C. *J. Fluid Mech.* **2011**, *666*, 146−154.
(19) Hodgson, K. T.; Berg, J. C. *J. Colloid Interface Sci.* **1988**, *121*, 22−31.
(20) Roberts, R.; Senden, T.; Knackstedt, M.; Lyne, M. *J. Pulp Pap. Sci.* **2003**, *29*, 123−131.
(21) Reed, C.; Wilson, N. *J. Phys. D: Appl. Phys.* **1993**, *26*, 1378.
(22) Fries, N.; Dreyer, M. *J. Colloid Interface Sci.* **2008**, *320*, 259−263.
(23) Reyssat, M.; Courbin, L.; Reyssat, E.; Stone, H. A. *J. Fluid Mech.* **2008**, *615*, 335−344.
(24) Xiao, J.; Stone, H. A.; Attinger, D. *Langmuir* **2012**, *28*, 4208−4212.
(25) Reyssat, M.; Sangne, L.; van Nierop, E.; Stone, H. *Europhys. Lett.* **2009**, *86*, 56002.
(26) Bal, K.; Fan, J.; Sarkar, M.; Ye, L. *Int. J. Heat Mass Transfer* **2011**, *54*, 3096−3099.
(27) Shou, D.; Ye, L.; Fan, J.; Fu, K. *Langmuir* **2013**, *30*, 149−155.
(28) Cai, J.; Yu, B. *Transp. Porous Med.* **2011**, *89*, 251−263.
(29) Wiklund, H. S.; Uesaka, T. *Phys. Rev. E* **2013**, *87*, 023006.
(30) Young, W.-B. *Colloids Surf. Physicochem. Eng. Aspects* **2004**, *234*, 123−128.
(31) Masoodi, R.; Pillai, K. *J. Porous Media* **2012**, *15*, 775−783.
(32) Mark, A.; Sandboge, R.; Berce, A.; Edelvik, F.; Glatt, E.; Rief, S.; Wieg-mann, A.; Fredlund, M.; Amini, J.; Lai, R. *Tappi J.* **2012**, *11*, 9−16.
(33) Fang, L.; Jiang, J.; Wang, J.; Deng, C. *J. Reinf. Plast. Compos.* **2014**, *33*, 1430−1440.
(34) Patro, D.; Bhattacharyya, S.; Jayaram, V. *J. Am. Ceram. Soc.* **2007**, *90*, 3040−3046.
(35) Masoodi, R.; Pillai, K. M.; Varanasi, P. P. *AIChE J.* **2007**, *53*, 2769−2782.
(36) Raux, P. S.; Cockenpot, H.; Ramaioli, M.; Quéré, D.; Clanet, C. *Langmuir* **2013**, *29*, 3636−3644.
(37) Shou, D.; Ye, L.; Fan, J.; Fu, K.; Mei, M.; Wang, H.; Chen, Q. *Langmuir* **2014**, *30*, 5448−5454.
(38) Baily, K. C. *The Elder Pliny's Chapters on Chemical Subjects*; Edward Arnold & Co.: London, U.K., 1929; Vol. 2, p 41.
(39) Dungchai, W.; Chailapakul, O.; Henry, C. S. *Analyst* **2011**, *136*, 77−82.
(40) Carrilho, E.; Martinez, A. W.; Whitesides, G. M. *Anal. Chem.* **2009**, *81*, 7091−7095.
(41) Yagoda, H. *Ind. Eng. Chem. Anal. Ed.* **1937**, *9*, 79−82.
(42) de Tarso Garcia, P.; Garcia Cardoso, T. M.; Garcia, C. D.; Carrilho, E.; Tomazelli Coltro, W. K. *RSC Adv.* **2014**, *4*, 37637−37644.
(43) Zhang, Y.; Zhou, C.; Nie, J.; Le, S.; Qin, Q.; Liu, F.; Li, Y.; Li, J. *Anal. Chem.* **2014**, *86*, 2005−2012.
(44) Songjaroen, T.; Dungchai, W.; Chailapakul, O.; Laiwattanapaisal, W. *Talanta* **2011**, *85*, 2587−2593.
(45) Noiphung, J.; Songjaroen, T.; Dungchai, W.; Henry, C. S.; Chailapakul, O.; Laiwattanapaisal, W. *Anal. Chim. Acta* **2013**, *788*, 39−45.
(46) Lu, Y.; Shi, W.; Jiang, L.; Qin, J.; Lin, B. *Electrophoresis* **2009**, *30*, 1497−1500.
(47) Ma, S.; Tang, Y.; Liu, J.; Wu, J. *Talanta* **2014**, *120*, 135−140.
(48) Renault, C.; Koehne, J.; Ricco, A. J.; Crooks, R. M. *Langmuir* **2014**, *30*, 7030−7036.
(49) Li, X.; Liu, X. *Microfluid. Nanofluid.* **2014**, *16*, 819−827.
(50) Abe, K.; Suzuki, K.; Citterio, D. *Anal. Chem.* **2008**, *80*, 6928−6934.
(51) Li, X.; Tian, J.; Garnier, G.; Shen, W. *Colloids Surf., B* **2010**, *76*, 564−570.
(52) Maejima, K.; Tomikawa, S.; Suzuki, K.; Citterio, D. *RSC Adv.* **2013**, *3*, 9258−9263.
(53) Yamada, K.; Takaki, S.; Komuro, N.; Suzuki, K.; Citterio, D. *Analyst* **2014**, *139*, 1637−1643.
(54) Wang, J.; Monton, M. R. N.; Zhang, X.; Filipe, C. D. M.; Pelton, R.; Brennan, J. D. *Lab Chip* **2014**, *14*, 691−695.
(55) Olkkonen, J.; Lehtinen, K.; Erho, T. *Anal. Chem.* **2010**, *82*, 10246−10250.
(56) Määttänen, A.; Fors, D.; Wang, S.; Valtakari, D.; Ihalainen, P.; Peltonen, J. *Sens. Actuators, B: Chem.* **2011**, *160*, 1404−1412.
(57) Wu, Y.; Xue, P.; Kang, Y.; Hui, K. M. *Anal. Chem.* **2013**, *85*, 8661−8668.
(58) Martinez, A. W.; Phillips, S. T.; Wiley, B. J.; Gupta, M.; Whitesides, G. M. *Lab Chip* **2008**, *8*, 2146−2150.
(59) OuYang, L.; Wang, C.; Du, F.; Zheng, T.; Liang, H. *RSC Adv.* **2014**, *4*, 1093−1101.
(60) Fenton, E. M.; Mascarenas, M. R.; López, G. P.; Sibbett, S. S. *ACS Appl. Mater. Interfaces* **2008**, *1*, 124−129.
(61) Fu, E.; Kauffman, P.; Lutz, B.; Yager, P. *Sens. Actuators, B: Chem.* **2010**, *149*, 325−328.
(62) Renault, C.; Li, X.; Fosdick, S. E.; Crooks, R. M. *Anal. Chem.* **2013**, *85*, 7976−7979.
(63) Nie, J.; Liang, Y.; Zhang, Y.; Le, S.; Li, D.; Zhang, S. *Analyst* **2013**, *138*, 671−676.
(64) Cassano, C. L.; Fan, Z. H. *Microfluid. Nanofluid.* **2013**, *15*, 173−181.
(65) Giokas, D. L.; Tsogas, G. Z.; Vlessidis, A. G. *Anal. Chem.* **2014**, *86*, 6202−6207.
(66) Glavan, A. C.; Martinez, R. V.; Maxwell, E. J.; Subramaniam, A. B.; Nunes, R. M.; Soh, S.; Whitesides, G. M. *Lab Chip* **2013**, *13*, 2922−2930.
(67) Evans, E.; Gabriel, E. F. M.; Coltro, W. K. T.; Garcia, C. D. *Analyst* **2014**, *139*, 2127−2132.
(68) Spicar-Mihalic, P.; Toley, B.; Houghtaling, J.; Liang, T.; Yager, P.; Fu, E. *J. Micromech. Microeng.* **2013**, *23*, 067003.
(69) Fridley, G. E.; Le, H.; Yager, P. *Anal. Chem.* **2014**, *86*, 6447−6453.
(70) Thuo, M. M.; Martinez, R. V.; Lan, W.-J.; Liu, X.; Barber, J.; Atkinson, M. B. J.; Bandarage, D.; Bloch, J.-F.; Whitesides, G. M. *Chem. Mater.* **2014**, *26*, 4230−4237.
(71) Curto, V. F.; Lopez-Ruiz, N.; Capitan-Vallvey, L. F.; Palma, A. J.; Benito-Lopez, F.; Diamond, D. *RSC Adv.* **2013**, *3*, 18811.
(72) Nurak, T.; Praphairaksit, N.; Chailapakul, O. *Talanta* **2013**, *114*, 291−296.
(73) Demirel, G.; Babur, E. *Analyst* **2014**, *139*, 2326−2331.
(74) Kwong, P.; Gupta, M. *Anal. Chem.* **2012**, *84*, 10129−10135.
(75) Chen, B.; Kwong, P.; Gupta, M. *ACS Appl. Mater. Interfaces* **2013**, *5*, 12701−12707.
(76) Kao, P.-K.; Hsu, C.-C. *Microfluid. Nanofluid.* **2014**, *16*, 811−818.

(77) Obeso, C. G.; Sousa, M. P.; Song, W.; Rodriguez-Pérez, M. A.; Bhushan, B.; Mano, J. F. *Colloids Surf. Physicochem. Eng. Aspects* **2013**, *416*, 51−55.
(78) Sousa, M. P.; Mano, J. F. *ACS Appl. Mater. Interfaces* **2013**, *5*, 3731−3737.
(79) Cai, L.; Wang, Y.; Wu, Y.; Xu, C.; Zhong, M.; Lai, H.; Huang, J. *Analyst* **2014**, *139*, 4593−4598.
(80) Böhm, A.; Gattermayer, M.; Trieb, C.; Schabel, S.; Fiedler, D.; Miletzky, F.; Biesalski, M. *Cellulose* **2013**, *20*, 467−483.
(81) He, Q.; Ma, C.; Hu, X.; Chen, H. *Anal. Chem.* **2013**, *85*, 1327−1331.
(82) Kao, P.-K.; Hsu, C.-C. *Anal. Chem.* **2014**, *86*, 8757−8762.
(83) Martinez, A. W.; Phillips, S. T.; Whitesides, G. M. *Proc. Natl. Acad. Sci. U.S.A.* **2008**, *105*, 19606−19611.
(84) Liu, H.; Crooks, R. M. *J. Am. Chem. Soc.* **2011**, *133*, 17564−17566.
(85) Rattanarat, P.; Dungchai, W.; Cate, D.; Volckens, J.; Chailapakul, O.; Henry, C. S. *Anal. Chem.* **2014**, *86*, 3555−3562.
(86) Gerbers, R.; Foellscher, W.; Chen, H.; Anagnostopoulos, C.; Faghri, M. *Lab Chip* **2014**, *14*, 4042−4049.
(87) Martinez, A. W.; Phillips, S. T.; Whitesides, G. M.; Carrilho, E. *Anal. Chem.* **2009**, *82*, 3−10.
(88) Mentele, M. M.; Cunningham, J.; Koehler, K.; Volckens, J.; Henry, C. S. *Anal. Chem.* **2012**, *84*, 4474−4480.
(89) Liu, W.; Cassano, C. L.; Xu, X.; Fan, Z. H. *Anal. Chem.* **2013**, *85*, 10270−10276.
(90) Liu, H.; Xiang, Y.; Lu, Y.; Crooks, R. M. *Angew. Chem.* **2012**, *124*, 7031−7034.
(91) Schilling, K. M.; Lepore, A. L.; Kurian, J. A.; Martinez, A. W. *Anal. Chem.* **2012**, *84*, 1579−1585.
(92) Martinez, A. W.; Phillips, S. T.; Nie, Z.; Cheng, C.-M.; Carrilho, E.; Wiley, B. J.; Whitesides, G. M. *Lab Chip* **2010**, *10*, 2499−2504.
(93) Fu, E.; Lutz, B.; Kauffman, P.; Yager, P. *Lab Chip* **2010**, *10*, 918−920.
(94) Noh, H.; Phillips, S. T. *Anal. Chem.* **2010**, *82*, 4181−4187.
(95) Tian, J.; Kannangara, D.; Li, X.; Shen, W. *Lab Chip* **2010**, *10*, 2258−2264.
(96) Toley, B. J.; McKenzie, B.; Liang, T.; Buser, J. R.; Yager, P.; Fu, E. *Anal. Chem.* **2013**, *85*, 11545−11552.
(97) Lutz, B.; Liang, T.; Fu, E.; Ramachandran, S.; Kauffman, P.; Yager, P. *Lab Chip* **2013**, *13*, 2840−2847.
(98) Houghtaling, J.; Liang, T.; Thiessen, G.; Fu, E. *Anal. Chem.* **2013**, *85*, 11201−11204.
(99) Jahanshahi-Anbuhi, S.; Henry, A.; Leung, V.; Sicard, C.; Pennings, K.; Pelton, R.; Brennan, J. D.; Filipe, C. D. *Lab Chip* **2014**, *14*, 229−236.
(100) Lewis, G. G.; Robbins, J. S.; Phillips, S. T. *Macromolecules* **2013**, *46*, 5177−5183.
(101) Lewis, G. G.; DiTucci, M. J.; Phillips, S. T. *Angew. Chem.* **2012**, *124*, 12879−12882.
(102) Lewis, G. G.; Robbins, J. S.; Phillips, S. T. *Chem. Commun.* **2014**, *50*, 5352−5354.
(103) Lewis, G. G.; Robbins, J. S.; Phillips, S. T. *Anal. Chem.* **2013**, *85*, 10432−10439.
(104) Renault, C.; Anderson, M. J.; Crooks, R. M. *J. Am. Chem. Soc.* **2014**, *136*, 4616−4623.
(105) Lutz, B. R.; Trinh, P.; Ball, C.; Fu, E.; Yager, P. *Lab Chip* **2011**, *11*, 4274−4278.
(106) Apilux, A.; Ukita, Y.; Chikae, M.; Chailapakul, O.; Takamura, Y. *Lab Chip* **2013**, *13*, 126−135.
(107) Li, X.; Zwanenburg, P.; Liu, X. *Lab Chip* **2013**, *13*, 2609−2614.
(108) Zhu, Y.; Xu, X.; Brault, N. D.; Keefe, A. J.; Han, X.; Deng, Y.; Xu, J.; Yu, Q.; Jiang, S. *Anal. Chem.* **2014**, *86*, 2871−2875.
(109) Guan, L.; Cao, R.; Tian, J.; McLiesh, H.; Garnier, G.; Shen, W. *Cellulose* **2013**, *21*, 717−727.
(110) Glavan, A. C.; Martinez, R. V.; Subramaniam, A. B.; Yoon, H. J.; Nunes, R. M. D.; Lange, H.; Thuo, M. M.; Whitesides, G. M. *Adv. Funct. Mater.* **2014**, *24*, 60−70.
(111) Gong, M. M.; Zhang, P.; MacDonald, B. D.; Sinton, D. *Anal. Chem.* **2014**, *86*, 8090−8097.
(112) Dossi, N.; Toniolo, R.; Piccin, E.; Susmel, S.; Pizzariello, A.; Bontempelli, G. *Electroanalysis* **2013**, *25*, 2515−2522.
(113) Santhiago, M.; Henry, C. S.; Kubota, L. T. *Electrochim. Acta* **2014**, *130*, 771−777.
(114) Yang, J.; Nam, Y.-G.; Lee, S.-K.; Kim, C.-S.; Koo, Y.-M.; Chang, W.-J.; Gunasekaran, S. *Sens. Actuators, B: Chem.* **2014**, *203*, 44−53.
(115) Dungchai, W.; Chailapakul, O.; Henry, C. S. *Anal. Chem.* **2009**, *81*, 5821−5826.
(116) Lan, W. J.; Maxwell, E. J.; Parolo, C.; Bwambok, D. K.; Subramaniam, A. B.; Whitesides, G. M. *Lab Chip* **2013**, *13*, 4103−4108.
(117) Nie, Z.; Nijhuis, C. A.; Gong, J.; Chen, X.; Kumachev, A.; Martinez, A. W.; Narovlyansky, M.; Whitesides, G. M. *Lab Chip* **2010**, *10*, 477−483.
(118) Santhiago, M.; Wydallis, J. B.; Kubota, L. T.; Henry, C. S. *Anal. Chem.* **2013**, *85*, 5233−5239.
(119) Santhiago, M.; Kubota, L. T. *Sens. Actuators, B: Chem.* **2013**, *177*, 224−230.
(120) Dossi, N.; Toniolo, R.; Impellizzieri, F.; Bontempelli, G. *J. Electroanal. Chem.* **2014**, *722*−*723*, 90−94.
(121) Dossi, N.; Toniolo, R.; Terzi, F.; Impellizzieri, F.; Bontempelli, G. *Electrochim. Acta* **2014**, *146*, 518−524.
(122) de Araujo, W. R.; Paixao, T. R. L. C. *Analyst* **2014**, *139*, 2742−2747.
(123) Lan, W.-J.; Zou, X. U.; Hamedi, M. M.; Hu, J.; Parolo, C.; Maxwell, E. J.; Bühlmann, P.; Whitesides, G. M. *Anal. Chem.* **2014**, *86*, 9548−9553.
(124) Liana, D. D.; Raguse, B.; Wieczorek, L.; Baxter, G. R.; Chuah, K.; Gooding, J. J.; Chow, E. *RSC Adv.* **2013**, *3*, 8683−8691.
(125) Cunningham, J. C.; Brenes, N. J.; Crooks, R. M. *Anal. Chem.* **2014**, *86*, 6166−6170.
(126) Fosdick, S. E.; Anderson, M. J.; Renault, C.; DeGregory, P. R.; Loussaert, J. A.; Crooks, R. M. *Anal. Chem.* **2014**, *86*, 3659−3666.
(127) Ge, L.; Wang, S.; Yu, J.; Li, N.; Ge, S.; Yan, M. *Adv. Funct. Mater.* **2013**, *23*, 3115−3123.
(128) Li, W.; Li, L.; Li, M.; Yu, J.; Ge, S.; Yan, M.; Song, X. *Chem. Commun. (Cambridge, U. K.)* **2013**, *49*, 9540−9542.
(129) Li, W.; Li, L.; Ge, S.; Song, X.; Ge, L.; Yan, M.; Yu, J. *Biosens. Bioelectron.* **2014**, *56*, 167−173.
(130) Ma, C.; Li, W.; Kong, Q.; Yang, H.; Bian, Z.; Song, X.; Yu, J.; Yan, M. *Biosens. Bioelectron.* **2014**, *63*, 7−13.
(131) Li, L.; Xu, J.; Zheng, X.; Ma, C.; Song, X.; Ge, S.; Yu, J.; Yan, M. *Biosens. Bioelectron.* **2014**, *61*, 76−82.
(132) Li, L.; Ma, C.; Kong, Q.; Li, W.; Zhang, Y.; Ge, S.; Yan, M.; Yu, J. *J. Mater. Chem. B* **2014**, *2*, 6669−6674.
(133) Apilux, A.; Siangproh, W.; Praphairaksit, N.; Chailapakul, O. *Talanta* **2012**, *97*, 388−394.
(134) Cai, L.; Wu, Y.; Xu, C.; Chen, Z. *J. Chem. Educ.* **2013**, *90*, 232−234.
(135) Hossain, S. M.; Brennan, J. D. *Anal. Chem.* **2011**, *83*, 8772−8778.
(136) Ratnarathorn, N.; Chailapakul, O.; Henry, C. S.; Dungchai, W. *Talanta* **2012**, *99*, 552−557.
(137) Rattanarat, P.; Dungchai, W.; Cate, D. M.; Siangproh, W.; Volckens, J.; Chailapakul, O.; Henry, C. S. *Anal. Chim. Acta* **2013**, *800*, 50−55.
(138) Songjaroen, T.; Dungchai, W.; Chailapakul, O.; Henry, C. S.; Laiwattanapaisal, W. *Lab Chip* **2012**, *12*, 3392−3398.
(139) Wang, W.; Wu, W. Y.; Wang, W.; Zhu, J. J. *J. Chromatogr., A* **2010**, *1217*, 3896−3899.
(140) Zhu, W.-J.; Feng, D.-Q.; Chen, M.; Chen, Z.-D.; Zhu, R.; Fang, H.-L.; Wang, W. *Sens. Actuators, B: Chem.* **2014**, *190*, 414−418.
(141) Breslauer, D. N.; Maamari, R. N.; Switz, N. A.; Lam, W. A.; Fletcher, D. A. *PLoS One* **2009**, *4*, e6320.
(142) Shen, L.; Hagen, J. A.; Papautsky, I. *Lab Chip* **2012**, *12*, 4240−4243.

(143) Martinez, A. W.; Phillips, S. T.; Carrilho, E.; Thomas, S. W., III; Sindi, H.; Whitesides, G. M. *Anal. Chem.* **2008**, *80*, 3699−3707.
(144) Doeven, E. H.; Barbante, G. J.; Kerr, E.; Hogan, C. F.; Endler, J. A.; Francis, P. S. *Anal. Chem.* **2014**, *86*, 2727−2732.
(145) Funes-Huacca, M.; Wu, A.; Szepesvari, E.; Rajendran, P.; Kwan-Wong, N.; Razgulin, A.; Shen, Y.; Kagira, J.; Campbell, R.; Derda, R. *Lab Chip* **2012**, *12*, 4269−4278.
(146) Veigas, B.; Jacob, J. M.; Costa, M. N.; Santos, D. S.; Viveiros, M.; Inacio, J.; Martins, R.; Barquinha, P.; Fortunato, E.; Baptista, P. V. *Lab Chip* **2012**, *12*, 4802−4808.
(147) Park, T. S.; Li, W.; McCracken, K. E.; Yoon, J. Y. *Lab Chip* **2013**, *13*, 4832−4840.
(148) Tsai, T.-T.; Shen, S.-W.; Cheng, C.-M.; Chen, C.-F. *Sci. Technol. Adv. Mater.* **2013**, *14*, 044404.
(149) Wei, Q.; Qi, H.; Luo, W.; Tseng, D.; Ki, S. J.; Wan, Z.; Göröcs, Z. n.; Bentolila, L. A.; Wu, T.-T.; Sun, R. *ACS Nano* **2013**, *7*, 9147−9155.
(150) Lee, S.; Oncescu, V.; Mancuso, M.; Mehta, S.; Erickson, D. *Lab Chip* **2014**, *14*, 1437−1442.
(151) Weaver, A. A.; Reiser, H.; Barstis, T.; Benvenuti, M.; Ghosh, D.; Hunckler, M.; Joy, B.; Koenig, L.; Raddell, K.; Lieberman, M. *Anal. Chem.* **2013**, *85*, 6453−6460.
(152) Yetisen, A. K.; Martinez-Hurtado, J. L.; Garcia-Melendrez, A.; da Cruz Vasconcellos, F.; Lowe, C. R. *Sens. Actuators, B: Chem.* **2014**, *196*, 156−160.
(153) Oncescu, V.; O'Dell, D.; Erickson, D. *Lab Chip* **2013**, *13*, 3232−3238.
(154) Coskun, A. F.; Nagi, R.; Sadeghi, K.; Phillips, S.; Ozcan, A. *Lab Chip* **2013**, *13*, 4231−4238.
(155) Oncescu, V.; Mancuso, M.; Erickson, D. *Lab Chip* **2014**, *14*, 759−763.
(156) Cardoso, L. P.; Dias, R. F.; Freitas, A. A.; Hungria, E. M.; Oliveira, R. M.; Collovati, M.; Reed, S. G.; Duthie, M. S.; Stefani, M. M. *BMC Infect. Dis.* **2013**, *13*, 497.
(157) Salles, M.; Meloni, G.; de Araujo, W.; Paixão, T. *Anal. Methods* **2014**, *6*, 2047−2052.
(158) Delaney, J. L.; Doeven, E. H.; Harsant, A. J.; Hogan, C. F. *Anal. Chim. Acta* **2013**, *790*, 56−60.
(159) Wei, Q.; Nagi, R.; Sadeghi, K.; Feng, S.; Yan, E.; Ki, S. J.; Caire, R.; Tseng, D.; Ozcan, A. *ACS Nano* **2014**, *8*, 1121−1129.
(160) Thom, N. K.; Lewis, G. G.; Yeung, K.; Phillips, S. T. *RSC Adv.* **2014**, *4*, 1334−1340.
(161) Fu, E. *Analyst* **2014**, *139*, 4750−4757.
(162) Phillips, S. T.; Lewis, G. G. *MRS Bull.* **2013**, *38*, 315−319.
(163) Fang, X.; Wei, S.; Kong, J. *Lab Chip* **2014**, *14*, 911−915.
(164) Hao, Y.; Chen, W.; Wang, L.; Zhou, B.; Zang, Q.; Chen, S.; Liu, Y.-N. *Anal. Methods* **2014**, *6*, 2478.
(165) Pollock, N. R.; McGray, S.; Colby, D. J.; Noubary, F.; Nguyen, H.; Nguyen, T. A.; Khormaee, S.; Jain, S.; Hawkins, K.; Kumar, S.; Rolland, J. P.; Beattie, P. D.; Chau, N. V.; Quang, V. M.; Barfield, C.; Tietje, K.; Steele, M.; Weigl, B. H. *PLoS One* **2013**, *8*, e75616.
(166) Zuk, R. F.; Ginsberg, V. K.; Houts, T.; Judith, R.; Merrick, H.; Ullman, E. F.; Fischer, M. M.; Sizto, C. C.; Stiso, S. N.; Litman, D. J. *Clin. Chem.* **1985**, *31*, 1144−1150.
(167) Cate, D. M.; Dungchai, W.; Cunningham, J. C.; Volckens, J.; Henry, C. S. *Lab Chip* **2013**, *13*, 2397−2404.
(168) Lou, S. C.; Patel, C.; Ching, S.; Gordon, J. *Clin. Chem.* **1993**, *39*, 619−624.
(169) Zhao, C.; Thuo, M. M.; Liu, X. *Sci. Technol. Adv. Mater.* **2013**, *14*, 054402.
(170) Rowe, A. A.; Bonham, A. J.; White, R. J.; Zimmer, M. P.; Yadgar, R. J.; Hobza, T. M.; Honea, J. W.; Ben-Yaacov, I.; Plaxco, K. W. *PLoS One* **2011**, *6*, e23783.
(171) Ramfos, I.; Vassiliadis, N.; Blionas, S.; Efstathiou, K.; Fragoso, A.; O'Sullivan, C. K.; Birbas, A. *Biosens. Bioelectron.* **2013**, *47*, 482−489.
(172) Nemiroski, A.; Christodouleas, D. C.; Hennek, J. W.; Kumar, A. A.; Maxwell, E. J.; Fernández-Abedul, M. T.; Whitesides, G. M. *Proc. Natl. Acad. Sci. U.S.A.* **2014**, *111*, 11984−11989.
(173) Kim, U.; Ghanbari, S.; Ravikumar, A.; Seubert, J.; Figueira, S. *IEEE J. Transl. Eng. Health Med.* **2013**, *1*, 1−7.
(174) Taudte, R. V.; Beavis, A.; Wilson-Wilde, L.; Roux, C.; Doble, P.; Blanes, L. *Lab Chip* **2013**, *13*, 4164−4172.
(175) Sechi, D.; Greer, B.; Johnson, J.; Hashemi, N. *Anal. Chem.* **2013**, *85*, 10733−10737.
(176) Pollock, N. R.; Rolland, J. P.; Kumar, S.; Beattie, P. D.; Jain, S.; Noubary, F.; Wong, V. L.; Pohlmann, R. A.; Ryan, U. S.; Whitesides, G. M. *Sci. Transl. Med.* **2012**, *4*, 152ra129.
(177) Chen, X.; Chen, J.; Wang, F.; Xiang, X.; Luo, M.; Ji, X.; He, Z. *Biosens. Bioelectron.* **2012**, *35*, 363−368.
(178) Zhou, M.; Yang, M.; Zhou, F. *Biosens. Bioelectron.* **2014**, *55*, 39−43.
(179) Bagherbaigi, S.; Córcoles, E. P.; Wicaksono, D. H. B. *Anal. Methods* **2014**, *6*, 7175.
(180) Koesdjojo, M. T.; Wu, Y.; Boonloed, A.; Dunfield, E. M.; Remcho, V. T. *Talanta* **2014**, *130*, 122−127.
(181) Yang, X.; Piety, N. Z.; Vignes, S. M.; Benton, M. S.; Kanter, J.; Shevkoplyas, S. S. *Clin. Chem.* **2013**, *59*, 1506−1513.
(182) Rohrman, B. A.; Richards-Kortum, R. R. *Lab Chip* **2012**, *12*, 3082−3088.
(183) Sajid, M.; Kawde, A.-N.; Daud, M. *J. Saudi Chem. Soc.* **2014**, DOI: 10.1016/j.jscs.2014.09.001.
(184) Tian, L.; Tadepalli, S.; Hyun Park, S.; Liu, K.-K.; Morrissey, J. J.; Kharasch, E. D.; Naik, R. R.; Singamaneni, S. *Biosens. Bioelectron.* **2014**, *59*, 208−215.
(185) Yan, J.; Liu, Y.; Wang, Y.; Xu, X.; Lu, Y.; Pan, Y.; Guo, F.; Shi, D. *Sens. Actuators, B: Chem.* **2014**, *197*, 129−136.
(186) Kavosi, B.; Hallaj, R.; Teymourian, H.; Salimi, A. *Biosens. Bioelectron.* **2014**, *59*, 389−396.
(187) Liu, W.; Yang, H.; Ding, Y.; Ge, S.; Yu, J.; Yan, M.; Song, X. *Analyst* **2014**, *139*, 251−258.
(188) Daniel, R. M.; Dunn, R. V.; Finney, J. L.; Smith, J. C. *Annu. Rev. Biophys. Biomol. Struct.* **2003**, *32*, 69−92.
(189) Li, L.; Li, W.; Yang, H.; Ma, C.; Yu, J.; Yan, M.; Song, X. *Electrochim. Acta* **2014**, *120*, 102−109.
(190) Su, M.; Ge, L.; Ge, S.; Li, N.; Yu, J.; Yan, M.; Huang, J. *Anal. Chim. Acta* **2014**, *847*, 1−9.
(191) Liu, F.; Ge, S.; Yu, J.; Yan, M.; Song, X. *Chem. Commun.* **2014**, *50*, 10315−10318.
(192) Su, M.; Ge, L.; Kong, Q.; Zheng, X.; Ge, S.; Li, N.; Yu, J.; Yan, M. *Biosens. Bioelectron.* **2015**, *63*, 232−239.
(193) Shi, Z.; Wu, X.; Gao, L.; Tian, Y.; Yu, L. *Anal. Methods* **2014**, *6*, 4446−4454.
(194) Rosa, A. M.; Louro, A. F.; Martins, S. A.; Inácio, J.; Azevedo, A. M.; Prazeres, D. M. F. *Anal. Chem.* **2014**, *86*, 4340−4347.
(195) Yildiz, U. H.; Alagappan, P.; Liedberg, B. *Anal. Chem.* **2012**, *84*, 820−824.
(196) Scida, K.; Li, B.; Ellington, A. D.; Crooks, R. M. *Anal. Chem.* **2013**, *85*, 9713−9720.
(197) Zhou, F.; Noor, M. O.; Krull, U. J. *Anal. Chem.* **2014**, *86*, 2719−2726.
(198) Wang, Y.; Ge, L.; Wang, P.; Yan, M.; Ge, S.; Li, N.; Yu, J.; Huang, J. *Lab Chip* **2013**, *13*, 3945−3955.
(199) Delaney, J. L.; Hogan, C. F.; Tian, J.; Shen, W. *Anal. Chem.* **2011**, *83*, 1300−1306.
(200) Ge, L.; Yu, J.; Ge, S.; Yan, M. *Anal. Bioanal. Chem.* **2014**, *406*, 5613−5630.
(201) Deng, L.; Zhang, L.; Shang, L.; Guo, S.; Wen, D.; Wang, F.; Dong, S. *Biosens. Bioelectron.* **2009**, *24*, 2273−2276.
(202) Forster, R. J.; Bertoncello, P.; Keyes, T. E. *Annu. Rev. Anal. Chem.* **2009**, *2*, 359−385.
(203) Richter, M. M. *Chem. Rev.* **2004**, *104*, 3003−3036.
(204) Feng, Q.-M.; Pan, J.; Zhang, H.-R.; Xu, J.-J.; Chen, H.-Y. *Chem. Commun.* **2014**.
(205) Xu, Y.; Lou, B.; Lv, Z.; Zhou, Z.; Zhang, L.; Wang, E. *Anal. Chim. Acta* **2013**, *763*, 20−27.
(206) Luo, S.; Xiao, H.; Yang, S.; Liu, C.; Liang, J.; Tang, Y. *Sens. Actuators, B: Chem.* **2014**, *194*, 325−331.

(207) Gu, W.; Xu, Y.; Lou, B.; Lyu, Z.; Wang, E. *Electrochem. Commun.* **2014**, *38*, 57−60.
(208) Krishnan, N.; Dickman, M. B.; Becker, D. F. *Free Radical Biol. Med.* **2008**, *44*, 671−681.
(209) Yan, J.; Yan, M.; Ge, L.; Yu, J.; Ge, S.; Huang, J. *Chem. Commun.* **2013**, *49*, 1383−1385.
(210) Yang, H.; Kong, Q.; Wang, S.; Xu, J.; Bian, Z.; Zheng, X.; Ma, C.; Ge, S.; Yu, J. *Biosens. Bioelectron.* **2014**, *61*, 21−27.
(211) Zhang, X.; Li, J.; Chen, C.; Lou, B.; Zhang, L.; Wang, E. *Chem. Commun.* **2013**, *49*, 3866−3868.
(212) Davaji, B.; Lee, C. H. *Biosens. Bioelectron.* **2014**, *59*, 120−126.
(213) Abbas, A.; Brimer, A.; Slocik, J. M.; Tian, L.; Naik, R. R.; Singamaneni, S. *Anal. Chem.* **2013**, *85*, 3977−3983.
(214) Liu, Q.; Wang, J.; Wang, B.; Li, Z.; Huang, H.; Li, C.; Yu, X.; Chu, P. K. *Biosens. Bioelectron.* **2014**, *54*, 128−134.
(215) Fobel, R.; Kirby, A. E.; Ng, A. H.; Farnood, R. R.; Wheeler, A. R. *Adv. Mater.* **2014**, *26*, 2838−2843.
(216) Choi, K.; Ng, A. H.; Fobel, R.; Wheeler, A. R. *Annu. Rev. Anal. Chem.* **2012**, *5*, 413−440.
(217) Díez-Gil, C.; Caballero, A.; Ratera, I.; Tárraga, A.; Molina, P.; Veciana, J. *Sensors* **2007**, *7*, 3481−3488.
(218) Li, L.; Xiang, H.; Zhou, X.; Li, M.; Wu, D. *J. Chem. Educ.* **2012**, *89*, 559−560.
(219) Pardasani, D.; Tak, V.; Purohit, A. K.; Dubey, D. K. *Analyst* **2012**, *137*, 5648−5653.
(220) Sameenoi, Y.; Panymeesamer, P.; Supalakorn, N.; Koehler, K.; Chailapakul, O.; Henry, C. S.; Volckens, J. *Environ. Sci. Technol.* **2013**, *47*, 932−940.
(221) Gu, Z.; Zhao, M.; Sheng, Y.; Bentolila, L. A.; Tang, Y. *Anal. Chem.* **2011**, *83*, 2324−2329.
(222) Lee, C. H.; Tian, L.; Singamaneni, S. *ACS Appl. Mater. Interfaces* **2010**, *2*, 3429−3435.
(223) Jayawardane, B. M.; Coo, d. L.; Cattrall, W. R.; Kolev, D. S. *Anal. Chim. Acta* **2013**, *803*, 106−112.
(224) Feng, L.; Li, X.; Li, H.; Yang, W.; Chen, L.; Guan, Y. *Anal. Chim. Acta* **2013**, *780*, 74−80.
(225) Cate, D. M.; Nanthasurasak, P.; Riwkulkajorn, P.; L'Orange, C.; Henry, C. S.; Volckens, J. *Ann. Occup. Hyg.* **2014**, met078.
(226) Bondarenko, O.; Juganson, K.; Ivask, A.; Kasemets, K.; Mortimer, M.; Kahru, A. *Arch. Toxicol.* **2013**, *87*, 1181−1200.
(227) Brewer, G. J. *J. Trace Elem. Med. Biol.* **2012**, *26*, 89−92.
(228) Li, S.-X.; Lin, X.; Zheng, F.; Liang, W.; Zhong, Y.; Cai, J.-B. *Anal. Chem.* **2014**.
(229) Wei, W. Y.; White, I. M. *Analyst* **2013**, *138*, 1020−1025.
(230) Chen, G.-H.; Chen, W.-Y.; Yen, Y.-C.; Wang, C.-W.; Chang, H.-T.; Chen, C.-F. *Anal. Chem.* **2014**, *86*, 6843−6849.
(231) Alkasir, R. S. J.; Ornatska, M.; Andreescu, S. *Anal. Chem.* **2012**, *84*, 9729−9737.
(232) Burnham, S.; Hu, J.; Anany, H.; Brovko, L.; Deiss, F.; Derda, R.; Griffiths, M. W. *Anal. Bioanal. Chem.* **2014**, *406*, 5685−5693.
(233) Kavruk, M.; Özalp, C. V.; Öktem, A. H. *J. Anal. Methods Chem.* **2013**, *2013*, 8.
(234) Jayawardane, B. M.; Wei, S.; McKelvie, I. D.; Kolev, S. D. *Anal. Chem.* **2014**, *86*, 7274−7279.
(235) Pesenti, A.; Taudte, R. V.; McCord, B.; Doble, P.; Roux, C.; Blanes, L. *Anal. Chem.* **2014**, *86*, 4707−4714.
(236) Lu, Q.; Collins, G. E.; Smith, M.; Wang, J. *Anal. Chim. Acta* **2002**, *469*, 253−260.
(237) Peters, K. L.; Corbin, I.; Kaufman, L. M.; Zreibe, K.; Blanes, L.; McCord, B. R. *Anal. Methods* **2014**, DOI: 10.1039/C4AY01677G.
(238) Dungchai, W.; Sameenoi, Y.; Chailapakul, O.; Volckens, J.; Henry, C. S. *Analyst* **2013**, *138*, 6766−6773.
(239) Bisha, B.; Adkins, J.; Jokerst, J.; Chandler, J.; Pérez-Méndez, A.; Coleman, S.; Sbodio, A.; Suslow, T.; Danyluk, M.; Henry, C.; Goodridge, L. D. *J. Vis. Exp.* **2014**, DOI: 10.3791/51414.
(240) Deiss, F.; Funes-Huacca, M. E.; Bal, J.; Tjhung, K. F.; Derda, R. *Lab Chip* **2014**, *14*, 167−171.
(241) Bauer, A.; Kirby, W.; Sherris, J. C.; Turck, M. *Am. J. Clin. Pathol.* **1966**, *45*, 493.
(242) Sun, G.; Wang, P.; Ge, S.; Ge, L.; Yu, J.; Yan, M. *Biosens. Bioelectron.* **2014**, *56*, 97−103.
(243) Kang, Q.; Yang, L.; Chen, Y.; Luo, S.; Wen, L.; Cai, Q.; Yao, S. *Anal. Chem.* **2010**, *82*, 9749−9754.
(244) Agency, U. E. P. National Primary Drinking Water Regulations, http://water.epa.gov/drink/contaminants/.
(245) Pohanish, R. P. *Sittig's Handbook of Toxic and Hazardous Chemicals and Carcinogens*, 5th ed.; William Andrew: Norwich, NY, 2008.
(246) Cui, J.; Lisak, G.; Strzalkowska, S.; Bobacka, J. *Analyst* **2014**, *139*, 2133−2136.
(247) Mensah, S. T.; Gonzalez, Y.; Calvo-Marzal, P.; Chumbimuni-Torres, K. Y. *Anal. Chem.* **2014**, *86*, 7269−7273.
(248) Mirasoli, M.; Buragina, A.; Dolci, L. S.; Guardigli, M.; Simoni, P.; Montoya, A.; Maiolini, E.; Girotti, S.; Roda, A. *Anal. Chim. Acta* **2012**, *721*, 167−172.
(249) Mani, V.; Kadimisetty, K.; Malla, S.; Joshi, A. A.; Rusling, J. F. *Environ. Sci. Technol.* **2013**, *47*, 1937−1944.
(250) Zhang, M.; Ge, L.; Ge, S.; Yan, M.; Yu, J.; Huang, J.; Liu, S. *Biosens. Bioelectron.* **2013**, *41*, 544−550.
(251) Jokerst, J. C.; Adkins, J. A.; Bisha, B.; Mentele, M. M.; Goodridge, L. D.; Henry, C. S. *Anal. Chem.* **2012**, *84*, 2900−2907.
(252) Wang, Y.; Ping, J.; Ye, Z.; Wu, J.; Ying, Y. *Biosens. Bioelectron.* **2013**, *49*, 492−498.
(253) Shi, J.; Tang, F.; Xing, H.; Zheng, H.; Lianhua, B.; Wei, W. *J. Brazil Chem. Soc.* **2012**, *23*, 1124−1130.
(254) Liu, W.; Kou, J.; Xing, H.; Li, B. *Biosens. Bioelectron.* **2014**, *52*, 76−81.
(255) Community Collaborative Rain, Hail & Snow Network.
(256) Conrad, C. C.; Hilchey, K. G. *Environ. Monit. Assess.* **2011**, *176*, 273−291.